

CERN-TH/99-34

hep-ph/9902371

February 1999

Higgs Bosons in the Minimal Supersymmetric Standard Model with Explicit CP Violation

Apostolos Pilaftsis and Carlos E.M. Wagner

Theory Division, CERN, CH-1211 Geneva 23, Switzerland

ABSTRACT

We study the Higgs-boson mass spectrum of the minimal supersymmetric standard model, in which the tree-level CP invariance of the Higgs potential is broken explicitly by loop effects of soft-CP-violating Yukawa interactions related to scalar quarks of the third generation. The analysis is performed by considering the CP-non-invariant renormalization-group improved effective potential through next-to-leading order that includes leading logarithms due to two-loop Yukawa and QCD corrections. We find that the three neutral Higgs particles predicted by the theory may strongly mix with one another, thereby significantly modifying their tree-level couplings to fermions and to the W^\pm and Z bosons. We analyze the phenomenological consequences of such a minimal supersymmetric scenario of explicit CP violation on the production rates of the lightest Higgs particle, and discuss strategies for its potential discovery at high-energy colliders.

1 Introduction

Despite the great phenomenological success of the minimal standard model (SM) at collider and lower energies, its full experimental vindication is not yet complete. The Higgs boson H , the ultimate cornerstone of the SM responsible for endowing the observed fermions and the W^\pm and Z bosons with masses, still remains elusive thus far. Recent experiments at the CERN Large Electron Positron Collider operating at energies of 189 GeV (LEP2) place a severe lower bound on M_H , i.e. $M_H \geq 95.5$ GeV at 95% confidence level (CL) [1]. On the other hand, global experimental data and theoretical analyses of radiative effects suggest that if nature indeed realizes the SM Higgs boson, it is then very unlikely that its mass be much larger than about 250 GeV [2]. Nevertheless, there are many theoretical reasons to believe that the SM represents the low-energy limit of a more fundamental theory whose first clear signals are expected to be seen in experiments accessing energies in the range of 0.1 to 1 TeV. Especially, supersymmetry (SUSY) appears theoretically to be a compelling ingredient for a successful unification of gravity with all other fundamental forces in nature by means of supergravity and superstrings. In its minimal realization, the minimal supersymmetric standard model (MSSM), SUSY must be broken softly, in agreement with experimental observations [3]. Unlike the SM, the MSSM offers an appealing solution to the gauge hierarchy problem, which is reflected by the perturbative stability of such a theory from the electroweak to the Planck energy scale. Because of the holomorphicity of the superpotential, the MSSM must contain at least two Higgs doublets, denoted as $\tilde{\Phi}_1$ and Φ_2 , with opposite hypercharges, $Y(\Phi_2) = -Y(\tilde{\Phi}_1) = 1$, so as to give tree-level masses to both up and down families, and to cancel the triangle anomalies.

Even though SUSY requires the presence of two Higgs doublets in the theory, the so-extended Higgs sector of the MSSM remains very predictive. This is because, at the tree level, all four-dimensional quartic couplings in the Higgs potential are not independent, but related to the known electroweak coupling constants g_w and g' of the gauge groups $SU(2)_L$ and $U(1)_Y$, respectively. The CP-conserving MSSM predicts three Higgs states: two of the Higgs bosons, h and H , are even under CP and the Higgs boson A has CP-odd parity. Beyond the Born approximation, extensive theoretical studies based on renormalization-group (RG) methods and diagrammatic techniques have shown [4,5,6] that the lightest CP-even Higgs boson, h , must possess a mass below 130 GeV. This upper bound is reached for large values of the ratio of Higgs vacuum expectation values, $\tan\beta \equiv \langle\Phi_2\rangle/\langle\tilde{\Phi}_1\rangle > 15$. For low values of $\tan\beta \approx 2$, the upper bound on the mass of h decreases substantially, i.e. $M_h \lesssim 110$ GeV. For such low $\tan\beta$ scenarios, the current experimental limit on M_h is almost equal to the SM Higgs-mass bound for large values of M_A , i.e. $M_h \geq 95$ GeV at 95%

CL, decreasing slightly for low values of M_A , of the order of the weak scale. Therefore, the present experimental bounds put strong restrictions on models with low values of $\tan\beta$, close to the infrared fixed-point value [7,8]. Therefore, next-round experiments at LEP2 turn out to be very crucial, as they can potentially exclude a significant portion of the parameter space of the CP-conserving MSSM [8].

Most analyses of the Higgs-boson mass spectrum of the MSSM have been performed, in the existing literature, only within the restricted framework of an effective CP-invariant Higgs potential. Recently, it has been shown [9], however, that the tree-level CP invariance of the MSSM Higgs sector can be broken sizeably by one-loop effects that involve trilinear CP-violating couplings of the scalar top and bottom quarks to the Higgs states. As a consequence, the high degree of the tree-level mass degeneracy between H and A may be considerably lifted at one loop. Within the context of general two-Higgs-doublet models, the latter possibility has been extensively discussed by several authors, in connection with observable phenomena of resonant CP violation through HA mixing [10] at future high-energy colliders, such as the Next Linear e^+e^- Collider (NLC) [11,12], the CERN Large Hadron Collider (LHC) [10,13] and the proposed First Muon Collider (FMC) [14,15]. Another important consequence of Higgs-sector CP violation in the MSSM is that the loop-induced CP-violating hA mixing can be of a size comparable to M_h , which may affect the predictions obtained for the mass of the lightest Higgs boson. CP violation and a light neutral Higgs boson are essential ingredients to account for the observed baryonic asymmetry in the Universe, through the mechanism of electroweak baryogenesis in the MSSM [16].

In this paper, we shall systematically study the mass spectrum of Higgs bosons in the MSSM with explicit CP violation. In such a scenario, both Higgs-boson masses and their couplings to fermions, W^\pm and Z bosons are significantly affected by the presence of CP-violating interactions. Therefore, we shall pay particular attention to the predictions obtained for the production rates of the lightest Higgs boson at LEP2 and other high-energy machines, such as the upgraded option of the Tevatron at Fermilab. Our analysis will be based on the computation of the CP-non-invariant RG-improved effective potential up to next-to-leading order. The dominant contributions to the effective potential come from the top (t) and bottom (b) quarks, as well as from their supersymmetric partners. For this purpose, we neglect chargino and neutralino quantum corrections. However, we include leading logarithms due to two-loop QCD and t and b Yukawa corrections [17,18]. As has been explicitly shown in [18,6], these corrections improve the effective Higgs potential by minimizing its scale dependence significantly.

CP-violating low-energy constraints, especially those coming from the electric dipole

moment (EDM) of the neutron and the electron, play an important role in our analysis [19,20,21,22,23,24,25]. However, there have been several suggestions to evade these constraints, without suppressing the CP-violating phases of the theory. One option is to make the first two generations of scalar fermions rather heavy, e.g. above 1 TeV [22]. Another possibility is to arrange for partial cancellations among the different EDM contributions [23]. Finally, it is possible to make the quantum corrections of the first two generations to EDMs negligible by requiring a kind of non-universality in the soft-trilinear Yukawa couplings [24]. Nevertheless, the aforementioned options do not prevent the supersymmetric analog of the two-loop Barr–Zee mechanism for generating EDMs from becoming large for high values of $\tan\beta$ [25]. Therefore, in our study, we shall consider these last ‘direct’ EDM constraints related to the CP-violating phases of scalar quarks of the third generation.

The organization of the paper is as follows: in Section 2 we consider the CP-violating RG-improved effective Higgs potential of the MSSM, and derive the minimization conditions related to the Higgs ground state. In addition, we calculate the general mass matrices of the neutral and charged Higgs bosons. Technical details are relegated to the Appendix. In Section 3 we compute the three mass eigenvalues of the (3×3) -dimensional mass matrix of the neutral Higgs bosons, and the respective mixing angles. In Section 4 we consider the effect of EDM constraints on the CP-violating parameters related to the third-generation scalar fermions. Section 5 discusses the interactions of the Higgs particles with fermions, and with the W^\pm and Z bosons in the presence of CP violation. Furthermore, we analyze the phenomenological implications of these interactions for Higgs-boson searches at LEP2, and discuss the prospects of probing such a minimal SUSY scenario of explicit CP violation at an upgraded Tevatron machine. Section 6 summarizes our conclusions.

2 The CP-violating Higgs potential of the MSSM

The MSSM introduces several new parameters in the theory that are absent from the SM and could, in principle, possess CP-odd phases [19]. Specifically, the new CP-odd phases may come from the following parameters: (i) the mass parameter μ , which involves the bilinear mixing of the two Higgs chiral superfields in the superpotential; (ii) the soft-SUSY-breaking gaugino masses m_λ , where λ collectively denotes \tilde{g} , \tilde{W} and \tilde{B} , i.e. the gauginos of the gauge groups $SU(3)_c$, $SU(2)_L$ and $U(1)_Y$, respectively; (iii) the soft bilinear Higgs-mixing mass m_{12}^2 , which is sometimes denoted as $B\mu$ in the literature; and (iv) the soft trilinear Yukawa couplings A_f of the Higgs particles to scalar fermions. If the universality condition is imposed on all gaugino masses at the unification scale M_X , then m_λ has a common phase. Likewise, the different trilinear couplings A_f are all equal at M_X , i.e.

$A_f = A$. Here, one may slightly deviate from exact universality by assuming that A is a matrix in the flavour space [24]. In particular, it has been argued recently [25] that many dangerously large contributions to the electron and neutron EDMs may naturally be avoided by choosing the trilinear coupling of the Higgs fields to the scalar quarks of the first and second generation to be much smaller than the one of the third generation, i.e. $A_f \simeq (0, 0, 1)A$.

It is known that the conformal-invariant part of the supersymmetric Lagrangian possesses two global Peccei–Quinn-type symmetries:

- (i) The $U(1)_Q$ symmetry, with Q assignments $Q(\hat{H}_1) = 1$, $Q(\hat{H}_2) = -2$, $Q(\hat{Q}) = Q(\hat{L}) = 0$, $Q(\hat{U}) = 2$ and $Q(\hat{D}) = Q(\hat{E}) = -1$, where the caret on the fields symbolizes superfields. \hat{H}_1 and \hat{H}_2 are the Higgs superfields, which have opposite hypercharges $Y(\hat{H}_2) = -Y(\hat{H}_1) = 1$, and \hat{Q} (\hat{L}), \hat{U} and \hat{D} (\hat{E}) are the chiral multiplets of the quark (lepton) left-handed doublet, the right-handed up quark and the right-handed down quark (lepton), respectively. The chiral multiplets carry the hypercharges: $Y(\hat{Q}) = 1/3$, $Y(\hat{L}) = -1$, $Y(\hat{U}) = -4/3$, $Y(\hat{D}) = 2/3$, and $Y(\hat{E}) = 2$. The $U(1)_Q$ symmetry is broken by the μ and m_{12}^2 parameters.
- (ii) The $U(1)_R$ symmetry acting on the Grassmann-valued coordinates θ and $\bar{\theta}$, i.e. $e^{i\alpha\theta}$ and $e^{-i\alpha\bar{\theta}}$. So, the θ coordinate of superspace carries charge 1. Moreover, all matter superfields carry charge 1 and all Higgs superfields carry charge 0. Under such a transformation, the gaugino fields carry charge 1. The superpotential carries charge 2. Consequently, this symmetry is broken by the Majorana masses of the gauginos as well as by the scalar-fermion–Higgs trilinear couplings A_f and the parameter μ .

As a consequence, not all phases of the four complex parameters $\{\mu, m_{12}^2, m_\lambda, A\}$ turn out to be physical [20], i.e. two phases may be removed by redefining the fields accordingly. Employing the global symmetries (i) and (ii), one of the Higgs doublets and the gaugino fields λ can be rephased in a way such that m_λ and m_{12}^2 become real numbers. As we will see, the fact that m_{12}^2 is made real complies also with the CP-odd tadpole constraint on the Higgs potential at the tree level [9]. Thus, $\arg(\mu)$ and $\arg(A)$ are the only physical CP-violating phases in the MSSM supplemented by universal boundary conditions at low energies.*

Denoting the scalar components of the Higgs superfields \hat{H}_1 and \hat{H}_2 by $\tilde{\Phi}_1 = i\tau_2\Phi_1^*$ (τ_2 is the usual Pauli matrix) and Φ_2 , the most general CP-violating Higgs potential of the

*Observe that, owing to the RG evolution, even starting with universal boundary conditions at high energies, the low-energy parameters tend to be non-universal.

MSSM may conveniently be described by the effective Lagrangian

$$\begin{aligned}
\mathcal{L}_V = & \mu_1^2(\Phi_1^\dagger\Phi_1) + \mu_2^2(\Phi_2^\dagger\Phi_2) + m_{12}^2(\Phi_1^\dagger\Phi_2) + m_{12}^{*2}(\Phi_2^\dagger\Phi_1) + \lambda_1(\Phi_1^\dagger\Phi_1)^2 + \lambda_2(\Phi_2^\dagger\Phi_2)^2 \\
& + \lambda_3(\Phi_1^\dagger\Phi_1)(\Phi_2^\dagger\Phi_2) + \lambda_4(\Phi_1^\dagger\Phi_2)(\Phi_2^\dagger\Phi_1) + \lambda_5(\Phi_1^\dagger\Phi_2)^2 + \lambda_5^*(\Phi_2^\dagger\Phi_1)^2 \\
& + \lambda_6(\Phi_1^\dagger\Phi_1)(\Phi_1^\dagger\Phi_2) + \lambda_6^*(\Phi_1^\dagger\Phi_1)(\Phi_2^\dagger\Phi_1) + \lambda_7(\Phi_2^\dagger\Phi_2)(\Phi_1^\dagger\Phi_2) + \lambda_7^*(\Phi_2^\dagger\Phi_2)(\Phi_2^\dagger\Phi_1).
\end{aligned} \tag{2.1}$$

At the tree level, the kinematic parameters are given by

$$\begin{aligned}
\mu_1^2 = & -m_1^2 - |\mu|^2, & \mu_2^2 = & -m_2^2 - |\mu|^2, & \lambda_1 = \lambda_2 = & -\frac{1}{8}(g_w^2 + g'^2), \\
\lambda_3 = & -\frac{1}{4}(g_w^2 - g'^2), & \lambda_4 = & \frac{1}{2}g_w^2, & \lambda_5 = \lambda_6 = \lambda_7 = & 0.
\end{aligned} \tag{2.2}$$

In Eqs. (2.1) and (2.2), m_1^2 , m_2^2 and m_{12}^2 are soft-SUSY-breaking parameters related to the Higgs sector. Beyond the Born approximation, the quartic couplings λ_5 , λ_6 , λ_7 receive significant radiative corrections from trilinear Yukawa couplings of the Higgs fields to scalar-top and scalar-bottom quarks. These parameters are in general complex. The analytic expressions of the quartic couplings are given in the appendix.

Our next step is to determine the ground state of the MSSM Higgs potential. To this end, we consider the linear decompositions of the Higgs fields

$$\Phi_1 = \begin{pmatrix} \phi_1^+ \\ \frac{1}{\sqrt{2}}(v_1 + \phi_1 + ia_1) \end{pmatrix}, \quad \Phi_2 = e^{i\xi} \begin{pmatrix} \phi_2^+ \\ \frac{1}{\sqrt{2}}(v_2 + \phi_2 + ia_2) \end{pmatrix}, \tag{2.3}$$

where v_1 and v_2 are the moduli of the vacuum expectation values (VEVs) of the Higgs doublets and ξ is their relative phase. Without any loss of generality, in the parameterization of the Higgs doublets in Eq. (2.3), we have adopted a weak basis in which the VEV v_1 (v_2) and the quantum fluctuation ϕ_1 (ϕ_2) have the same phase. Furthermore, we assume the absence of any CP-odd component due to spontaneous CP violation [26]. Although radiative corrections can, in principle, lead to a spontaneous breakdown of CP invariance in the MSSM [27], such a particular scenario, however, predicts an unacceptably small mass for the CP-odd Higgs scalar A , i.e. $M_A < 40$ GeV, and it is therefore ruled out experimentally [28,29].

The VEVs v_1 and v_2 and the phase ξ can now be determined by the minimization conditions on \mathcal{L}_V . This is achieved by requiring that the following tadpole parameters vanish:

$$\begin{aligned}
T_{\phi_1} \equiv \langle \frac{\partial \mathcal{L}_V}{\partial \phi_1} \rangle = & v c_\beta \left\{ \mu_1^2 + \text{Re}(m_{12}^2 e^{i\xi}) \tan \beta + v^2 \left[\lambda_1 c_\beta^2 + \frac{1}{2}(\lambda_3 + \lambda_4) s_\beta^2 \right. \right. \\
& \left. \left. + \text{Re}(\lambda_5 e^{2i\xi}) s_\beta^2 + \frac{3}{2} \text{Re}(\lambda_6 e^{i\xi}) s_\beta c_\beta + \frac{1}{2} \text{Re}(\lambda_7 e^{i\xi}) s_\beta^2 \tan \beta \right] \right\},
\end{aligned} \tag{2.4}$$

$$\begin{aligned}
T_{\phi_2} &\equiv \left\langle \frac{\partial \mathcal{L}_V}{\partial \phi_2} \right\rangle = v s_\beta \left\{ \mu_2^2 + \text{Re}(m_{12}^2 e^{i\xi}) \cot \beta + v^2 \left[\lambda_2 s_\beta^2 + \frac{1}{2} (\lambda_3 + \lambda_4) c_\beta^2 \right. \right. \\
&\quad \left. \left. + \text{Re}(\lambda_5 e^{2i\xi}) c_\beta^2 + \frac{1}{2} \text{Re}(\lambda_6 e^{i\xi}) c_\beta^2 \cot \beta + \frac{3}{2} \text{Re}(\lambda_7 e^{i\xi}) s_\beta c_\beta \right] \right\}, \tag{2.5}
\end{aligned}$$

$$\begin{aligned}
T_{a_1} &\equiv \left\langle \frac{\partial \mathcal{L}_V}{\partial a_1} \right\rangle = v s_\beta \left[\text{Im}(m_{12}^2 e^{i\xi}) + \text{Im}(\lambda_5 e^{2i\xi}) v^2 s_\beta c_\beta + \frac{1}{2} \text{Im}(\lambda_6 e^{i\xi}) v^2 c_\beta^2 \right. \\
&\quad \left. + \frac{1}{2} \text{Im}(\lambda_7 e^{i\xi}) v^2 s_\beta^2 \right], \tag{2.6}
\end{aligned}$$

$$\begin{aligned}
T_{a_2} &\equiv \left\langle \frac{\partial \mathcal{L}_V}{\partial a_2} \right\rangle = -v c_\beta \left[\text{Im}(m_{12}^2 e^{i\xi}) + \text{Im}(\lambda_5 e^{2i\xi}) v^2 s_\beta c_\beta + \frac{1}{2} \text{Im}(\lambda_6 e^{i\xi}) v^2 c_\beta^2 \right. \\
&\quad \left. + \frac{1}{2} \text{Im}(\lambda_7 e^{i\xi}) v^2 s_\beta^2 \right], \tag{2.7}
\end{aligned}$$

where $s_x \equiv \sin x$, $c_x \equiv \cos x$, $\tan \beta = v_2/v_1$ and $v^2 = v_1^2 + v_2^2$. Furthermore, we assume the absence of charge-breaking minima, i.e. variations of \mathcal{L}_V with respect to ϕ_1^+ and ϕ_2^+ vanish identically. It is now easy to see that the orthogonal rotation of the CP-odd fields,

$$\begin{pmatrix} a_1 \\ a_2 \end{pmatrix} = \begin{pmatrix} \cos \beta & -\sin \beta \\ \sin \beta & \cos \beta \end{pmatrix} \begin{pmatrix} G^0 \\ a \end{pmatrix}, \tag{2.8}$$

gives rise to a flat direction of the Higgs potential with respect to the G^0 field, i.e. $\langle \partial \mathcal{L}_V / \partial G^0 \rangle = 0$. In the newly defined weak basis, the G^0 field becomes the would-be Goldstone boson, which is absorbed by the longitudinal component of the Z boson. Moreover, the orthogonal rotation (2.8) of the CP-odd fields yields a non-trivial CP-odd tadpole parameter:

$$\begin{aligned}
T_a &\equiv \left\langle \frac{\partial \mathcal{L}_V}{\partial a} \right\rangle = -v \left[\text{Im}(m_{12}^2 e^{i\xi}) + \text{Im}(\lambda_5 e^{2i\xi}) v^2 s_\beta c_\beta + \frac{1}{2} \text{Im}(\lambda_6 e^{i\xi}) v^2 c_\beta^2 \right. \\
&\quad \left. + \frac{1}{2} \text{Im}(\lambda_7 e^{i\xi}) v^2 s_\beta^2 \right]. \tag{2.9}
\end{aligned}$$

In the CP-invariant limit of the theory, both T_a and the phase ξ vanish. Since m_{12}^2 is taken to be real at the tree level, a non-zero value of the phase ξ is first generated at the one-loop level [9]. Nevertheless, in a general two-Higgs-doublet model with Higgs-sector CP violation, the phase ξ already occurs in the Born approximation. For the sake of generality, we shall keep the full ξ dependence in the analytic results.

It is now interesting to discuss the conditions under which the Higgs sector of the MSSM respects the CP symmetry. We find that the CP invariance of the Higgs potential is assured only if

$$\text{Im}(m_{12}^4 \lambda_5^*) = \text{Im}(m_{12}^2 \lambda_6^*) = \text{Im}(m_{12}^2 \lambda_7^*) = 0. \tag{2.10}$$

If we assume a kind of universality between the trilinear Yukawa couplings at low energies, $A = A_t = A_b$, and neglect the small chargino and neutralino contributions, the phases of

the quartic couplings λ_5 , λ_6 and λ_7 are then related to one another. Employing the analytic results of the quartic couplings given in the Appendix, it is easy to show that

$$\text{Im}(\lambda_5^* \lambda_6^2) = \text{Im}(\lambda_5^* \lambda_7^2) = 0. \quad (2.11)$$

However, even in this case, the phase of the complex soft parameter m_{12}^2 is not restricted by any universal boundary condition imposed by minimal supergravity models at the unification point. In other words, the CP invariance of the Higgs potential of the MSSM holds true only if the condition

$$\text{Im}(m_{12}^{*2} \mu A) = 0 \quad (2.12)$$

is satisfied. Within the most general framework of the MSSM, the equality (2.12) [or equivalently (2.10)] can be violated, thus giving rise to observable CP violation.

CP violation in the Higgs potential of the MSSM leads to mixing mass terms between the CP-even and CP-odd Higgs fields [9]. Thus, one has to consider a (4×4) -dimensional mass matrix for the neutral Higgs bosons. In the weak basis (G^0, a, ϕ_1, ϕ_2) , the neutral Higgs-boson mass matrix \mathcal{M}_0^2 may be cast into the form

$$\mathcal{M}_0^2 = \begin{pmatrix} \widehat{\mathcal{M}}_P^2 & \mathcal{M}_{PS}^2 \\ \mathcal{M}_{SP}^2 & \mathcal{M}_S^2 \end{pmatrix}, \quad (2.13)$$

where $\widehat{\mathcal{M}}_P^2$ and \mathcal{M}_S^2 describe the CP-conserving transitions $(G^0, a) \rightarrow (G^0, a)$ and $(\phi_1, \phi_2) \rightarrow (\phi_1, \phi_2)$, respectively, and $\mathcal{M}_{PS}^2 = (\mathcal{M}_{SP}^2)^T$ contains the CP-violating mixings $(G^0, a) \leftrightarrow (\phi_1, \phi_2)$. The analytic form of the submatrices is given by

$$\widehat{\mathcal{M}}_P^2 = \begin{pmatrix} -\frac{c_\beta T_{\phi_1} + s_\beta T_{\phi_2}}{v} & \frac{s_\beta T_{\phi_1} - c_\beta T_{\phi_2}}{v} \\ \frac{s_\beta T_{\phi_1} - c_\beta T_{\phi_2}}{v} & M_a^2 - \frac{s_\beta \tan \beta T_{\phi_1} + c_\beta \cot \beta T_{\phi_2}}{v} \end{pmatrix}, \quad (2.14)$$

$$\mathcal{M}_{SP}^2 = v^2 \begin{pmatrix} 0 & \text{Im}(\lambda_5 e^{2i\xi}) s_\beta + \text{Im}(\lambda_6 e^{i\xi}) c_\beta \\ 0 & \text{Im}(\lambda_5 e^{2i\xi}) c_\beta + \text{Im}(\lambda_7 e^{i\xi}) s_\beta \end{pmatrix} - \frac{T_a}{v} \begin{pmatrix} s_\beta & c_\beta \\ -c_\beta & s_\beta \end{pmatrix}, \quad (2.15)$$

$$\mathcal{M}_S^2 = M_a^2 \begin{pmatrix} s_\beta^2 & -s_\beta c_\beta \\ -s_\beta c_\beta & c_\beta^2 \end{pmatrix} - \begin{pmatrix} \frac{T_{\phi_1}}{v c_\beta} & 0 \\ 0 & \frac{T_{\phi_2}}{v s_\beta} \end{pmatrix} \quad (2.16)$$

$$- v^2 \begin{pmatrix} 2\lambda_1 c_\beta^2 + 2\text{Re}(\lambda_5 e^{2i\xi}) s_\beta^2 + 2\text{Re}(\lambda_6 e^{i\xi}) s_\beta c_\beta & \lambda_{34} s_\beta c_\beta + \text{Re}(\lambda_6 e^{i\xi}) c_\beta^2 + \text{Re}(\lambda_7 e^{i\xi}) s_\beta^2 \\ \lambda_{34} s_\beta c_\beta + \text{Re}(\lambda_6 e^{i\xi}) c_\beta^2 + \text{Re}(\lambda_7 e^{i\xi}) s_\beta^2 & 2\lambda_2 s_\beta^2 + 2\text{Re}(\lambda_5 e^{2i\xi}) c_\beta^2 + 2\text{Re}(\lambda_7 e^{i\xi}) s_\beta c_\beta \end{pmatrix}.$$

In Eqs. (2.14) and (2.16), we have used the abbreviations $\lambda_{34} = \lambda_3 + \lambda_4$ and

$$M_a^2 = \frac{1}{s_\beta c_\beta} \left\{ \text{Re}(m_{12}^2 e^{i\xi}) + v^2 \left[2\text{Re}(\lambda_5 e^{2i\xi}) s_\beta c_\beta + \frac{1}{2} \text{Re}(\lambda_6 e^{i\xi}) c_\beta^2 + \frac{1}{2} \text{Re}(\lambda_7 e^{i\xi}) s_\beta^2 \right] \right\}. \quad (2.17)$$

If the MSSM is invariant under the CP symmetry, M_a is then the physical mass of the CP-odd Higgs scalar [5].

Correspondingly, the charged Higgs-boson mass matrix $\widehat{\mathcal{M}}_{\pm}^2$, spanned in the mass basis (G^{\pm}, H^{\pm}) , may be obtained by the Lagrangian

$$\mathcal{L}_{\text{mass}}^{\pm} = -(G^+, H^+) \widehat{\mathcal{M}}_{\pm}^2 \begin{pmatrix} G^- \\ H^- \end{pmatrix}, \quad (2.18)$$

with

$$\widehat{\mathcal{M}}_{\pm}^2 = \begin{pmatrix} -\frac{c_{\beta}T_{\phi_1} + s_{\beta}T_{\phi_2}}{v} & \frac{s_{\beta}T_{\phi_1} - c_{\beta}T_{\phi_2}}{v} - i\frac{T_a}{v} \\ \frac{s_{\beta}T_{\phi_1} - c_{\beta}T_{\phi_2}}{v} + i\frac{T_a}{v} & M_{H^{\pm}}^2 - \frac{s_{\beta}\tan\beta T_{\phi_1} + c_{\beta}\cot\beta T_{\phi_2}}{v} \end{pmatrix} \quad (2.19)$$

and

$$M_{H^{\pm}}^2 = \frac{1}{s_{\beta}c_{\beta}} \left\{ \text{Re}(m_{12}^2 e^{i\xi}) + v^2 \left[\frac{1}{2} \lambda_4 s_{\beta} c_{\beta} + \text{Re}(\lambda_5 e^{2i\xi}) s_{\beta} c_{\beta} + \frac{1}{2} \text{Re}(\lambda_6 e^{i\xi}) c_{\beta}^2 + \frac{1}{2} \text{Re}(\lambda_7 e^{i\xi}) s_{\beta}^2 \right] \right\}. \quad (2.20)$$

From Eqs. (2.17) and (2.20), we observe that $M_{H^{\pm}}^2$ is related to the mass of the would-be CP-odd Higgs scalar M_a^2 through

$$M_a^2 = M_{H^{\pm}}^2 - \frac{1}{2} \lambda_4 v^2 + \text{Re}(\lambda_5 e^{2i\xi}) v^2. \quad (2.21)$$

Taking this very last relation into account, we may express the neutral Higgs-boson masses as functions of M_{H^+} , μ , A_t , A_b , the common SUSY scale M_{SUSY} , $\tan\beta$ and the physical phase ξ . Since we neglect chargino and neutralino contributions, we can absorb the radiatively induced phase ξ into the definition of the μ parameter.

It is worth stressing that, even though CP violation decouples from the sector of the lightest Higgs boson for large values of $M_{H^+} \approx M_a$, this decoupling property of CP non-conservation does not generally persist for the system of the two heaviest Higgs bosons. This point may formally be seen as follows: in the large M_a^2 limit, assuming that the quartic couplings are kept fixed, the submatrix \mathcal{M}_S^2 given in Eq. (2.16) has one mass eigenvalue which approaches M_a^2 , and corresponds to the heaviest CP-even Higgs boson, while the other one is small at the electroweak scale, related to the lightest CP-even Higgs boson. Furthermore, the submatrix $\widehat{\mathcal{M}}_P^2$ in Eq. (2.14) has only one non-zero mass eigenvalue equal to M_a^2 , corresponding to the mass of the would-be CP-odd Higgs scalar. Thus, for large M_a^2 values, it is easy to see that the effective (2×2) -dimensional submatrix, which may be formed by the would-be CP-odd and the heaviest CP-even Higgs bosons, also contains

off-diagonal CP-violating terms coming from M_{SP}^2 in Eq. (2.15). These off-diagonal CP-violating matrix elements are generically of the order of the difference of the diagonal entries of the effective submatrix, thereby giving rise to a strong mixed system of CP violation. As we will see in Section 5, numerical estimates of CP violation in the heavy Higgs sector offer firm support of this observation.

3 Higgs-boson masses and mixing angles

In this section, we shall evaluate the physical masses of the neutral Higgs bosons and the mixing angles related to the diagonalization of the general 4×4 matrix \mathcal{M}_0^2 in Eq. (2.13). Even though our primary interest is in the CP-violating MSSM, the validity of the analytic expressions that we shall derive here extends to the most general class of CP-violating two-Higgs-doublet models. After setting all tadpole parameters to zero, we easily see that G^0 does not mix with the other neutral fields and so becomes an independent massless field, as it should be on account of the Goldstone theorem [9]. Then, \mathcal{M}_0^2 effectively reduces to a (3×3) -dimensional matrix, \mathcal{M}_N^2 , which is spanned in the weak basis (a, ϕ_1, ϕ_2) .

The mass eigenvalues of \mathcal{M}_N^2 are obtained by solving the characteristic equation of cubic order

$$x^3 + rx^2 + sx + t = 0, \quad (3.1)$$

with

$$\begin{aligned} r &= -\text{Tr}(\mathcal{M}_N^2), \\ s &= \frac{1}{2} [\text{Tr}^2(\mathcal{M}_N^2) - \text{Tr}(\mathcal{M}_N^4)], \\ t &= -\det(\mathcal{M}_N^2). \end{aligned} \quad (3.2)$$

To this end, it proves useful to define the following auxiliary parameters:

$$\begin{aligned} p &= \frac{3s - r^2}{3}, \\ q &= \frac{2r^3}{27} - \frac{rs}{3} + t, \\ D &= \frac{p^3}{27} + \frac{q^2}{4}. \end{aligned} \quad (3.3)$$

To ensure that the three eigenvalues are positive, it is necessary and sufficient to require that

$$D < 0, \quad r < 0, \quad s > 0, \quad t < 0. \quad (3.4)$$

Imposing these inequalities on the kinematic parameters of the theory, we may express the three mass eigenvalues of \mathcal{M}_N^2 as

$$\begin{aligned}\rho_1^2 &= -\frac{1}{3}r + 2\sqrt{-p/3} \cos\left(\frac{\varphi}{3}\right), \\ \rho_2^2 &= -\frac{1}{3}r + 2\sqrt{-p/3} \cos\left(\frac{\varphi}{3} + \frac{2\pi}{3}\right), \\ \rho_3^2 &= -\frac{1}{3}r + 2\sqrt{-p/3} \cos\left(\frac{\varphi}{3} - \frac{2\pi}{3}\right),\end{aligned}\tag{3.5}$$

with

$$\varphi = \arccos\left(-\frac{q}{2\sqrt{-p^3/27}}\right).\tag{3.6}$$

Since the Higgs-boson mass matrix \mathcal{M}_N^2 is symmetric, we can diagonalize it by means of an orthogonal rotation O as follows:

$$O^T \mathcal{M}_N^2 O = \text{diag}(M_{H_3}^2, M_{H_2}^2, M_{H_1}^2).\tag{3.7}$$

Note that some arbitrariness exists in assigning the mass eigenvalues ρ_1 , ρ_2 and ρ_3 in Eq. (3.5) to those related to the mass eigenfields H_1 , H_2 and H_3 in Eq. (3.7). For clarity of the presentation, we define these fields such that

$$M_{H_1} \leq M_{H_2} \leq M_{H_3}.\tag{3.8}$$

Alternatively, these fields could be defined in such a way that we have, in the CP-invariant limit of the theory, $H_1 \equiv h$, $H_2 \equiv H$, $H_3 \equiv A$, where h and H denote the lightest and heaviest CP-even Higgs bosons, respectively, and A is the CP-odd Higgs scalar. However, we should use the former definition, as the latter often leads to discontinuities in the H_i mass values, when plotted as a function of the MSSM parameters.

In general, the orthogonal matrix O in Eq. (3.7) can be described in terms of the three physical Euler-type angles χ , ψ and θ . We parameterize O , assuming $\chi, \psi \rightarrow 0$ or $\pi/2$ in the CP-conserving limit of the theory, as follows:

$$O = \begin{pmatrix} c_\chi c_\psi & -s_\chi c_\theta - s_\psi c_\chi s_\theta & s_\chi s_\theta - s_\psi c_\chi c_\theta \\ s_\chi c_\psi & c_\chi c_\theta - s_\psi s_\chi s_\theta & -c_\chi s_\theta - s_\psi s_\chi c_\theta \\ s_\psi & s_\theta c_\psi & c_\theta c_\psi \end{pmatrix}.\tag{3.9}$$

It is convenient to find first the entries O_{ij} , and then determine the three rotational angles by the obvious relations:

$$\psi = \arcsin(O_{31}), \quad \chi = \arcsin\left(\frac{O_{21}}{\cos\psi}\right), \quad \theta = \arcsin\left(\frac{O_{32}}{\cos\psi}\right),\tag{3.10}$$

where the mixing angles take on values in the interval $(-\pi/2, \pi/2]$.

If M_{ij}^2 , with $i, j = 1, 2, 3$, denote the matrix elements of \mathcal{M}_N^2 , the elements O_{ij} can then be obtained by appropriately solving the underdetermined coupled system of equations, $\sum_k M_{ik}^2 O_{kj} = M_{H(4-j)}^2 O_{ij}$:

$$\begin{aligned} (M_{11}^2 - M_{H(4-i)}^2)O_{1i} + M_{12}^2 O_{2i} + M_{13}^2 O_{3i} &= 0, \\ M_{21}^2 O_{1i} + (M_{22}^2 - M_{H(4-i)}^2)O_{2i} + M_{23}^2 O_{3i} &= 0, \\ M_{31}^2 O_{1i} + M_{32}^2 O_{2i} + (M_{33}^2 - M_{H(4-i)}^2)O_{3i} &= 0. \end{aligned} \quad (3.11)$$

More explicitly, we have

$$O = \begin{pmatrix} |x_1|/\Delta_1 & x_2/\Delta_2 & x_3/\Delta_3 \\ y_1/\Delta_1 & |y_2|/\Delta_2 & y_3/\Delta_3 \\ z_1/\Delta_1 & z_2/\Delta_2 & |z_3|/\Delta_3 \end{pmatrix}, \quad (3.12)$$

where

$$\Delta_i = \sqrt{x_i^2 + y_i^2 + z_i^2} \quad (3.13)$$

and

$$\begin{aligned} |x_1| &= \left\| \begin{array}{cc} M_{22}^2 - M_{H_3}^2 & M_{23}^2 \\ M_{32}^2 & M_{33}^2 - M_{H_3}^2 \end{array} \right\|, \quad y_1 = s_{x_1} \left| \begin{array}{cc} M_{23}^2 & M_{21}^2 \\ M_{33}^2 - M_{H_3}^2 & M_{31}^2 \end{array} \right|, \quad z_1 = s_{x_1} \left| \begin{array}{cc} M_{21}^2 & M_{22}^2 - M_{H_3}^2 \\ M_{31}^2 & M_{32}^2 \end{array} \right|, \\ x_2 &= s_{y_2} \left| \begin{array}{cc} M_{13}^2 & M_{12}^2 \\ M_{33}^2 - M_{H_2}^2 & M_{32}^2 \end{array} \right|, \quad |y_2| = \left\| \begin{array}{cc} M_{11}^2 - M_{H_2}^2 & M_{13}^2 \\ M_{31}^2 & M_{33}^2 - M_{H_2}^2 \end{array} \right\|, \quad z_2 = s_{y_2} \left| \begin{array}{cc} M_{12}^2 & M_{11}^2 - M_{H_2}^2 \\ M_{32}^2 & M_{31}^2 \end{array} \right|, \\ x_3 &= s_{z_3} \left| \begin{array}{cc} M_{12}^2 & M_{13}^2 \\ M_{22}^2 - M_{H_1}^2 & M_{23}^2 \end{array} \right|, \quad y_3 = s_{z_3} \left| \begin{array}{cc} M_{13}^2 & M_{11}^2 - M_{H_1}^2 \\ M_{23}^2 & M_{21}^2 \end{array} \right|, \quad |z_3| = \left\| \begin{array}{cc} M_{11}^2 - M_{H_1}^2 & M_{12}^2 \\ M_{21}^2 & M_{22}^2 - M_{H_1}^2 \end{array} \right\|. \end{aligned} \quad (3.14)$$

In Eq. (3.14), we have used the abbreviation $s_x \equiv \text{sign}(x)$, which is an operation that simply gives the sign of a real expression x . Notice that the parameterization of O in terms of x_i, y_i, z_i may be chosen, in a way such that indefinite expressions do not occur in the CP-conserving limit of the theory.

4 EDM constraints

As we mentioned in the introduction, the EDM of the electron and the neutron provide the most stringent constraints on the CP-violating parameters of the MSSM [19,20,21,22,23,24,25]. There have been several suggestions to suppress the EDM contributions coming from the first two families of scalar quarks without making the CP-violating

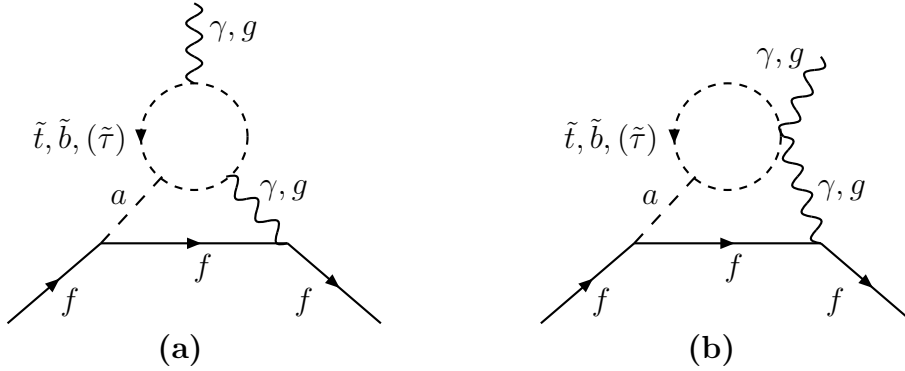


Figure 1: Two-loop contribution to EDM and CEDM of a light fermion f in the CP-violating MSSM (mirror-symmetric graphs are not shown). Note that $\tilde{\tau}$ does not contribute to the CEDM of a coloured fermion f .

phases of the theory very small [22,23,24,25]. To be specific, the following three possibilities may be considered: one can make the first two families of scalar fermions rather heavy, having a mass of order few TeV [22]. Another option is to arrange for partial cancellations among the different EDM contributions [23]. In this case, the CP-violating phases of the theory turn out to be rather correlated. Finally, an interesting alternative is to adopt a slightly non-universal scenario for the trilinear couplings A_f [24,25]. In particular, one may require that $\arg(\mu) < 10^{-2}$ and $A_f = (0, 0, 1)A$ [25]. In the latter scheme, $A_\tau = A_t = A_b$ are the only large trilinear couplings in the theory with CP-violating phases of order unity. Furthermore, assuming that gluinos are heavier than about 400 GeV [23], one may significantly reduce the size of the EDM effect due to Weinberg's three-gluon operator [30] well below the present experimental bound.

In the aforementioned SUSY scenarios, however, the two-loop Barr-Zee-type [31] contribution to the electron and neutron EDMs, shown in Fig. 1, can still be potentially large [25]. It is important to notice that the very same kind of loop graphs generated by scalar top and bottom quarks are also responsible for CP violation in the Higgs sector of the MSSM. Therefore, we are compelled to take these two-loop EDM constraints into consideration. The graphs displayed in Fig. 1 give rise to both an EDM (d_f/e) and a chromo-EDM (CEDM) (d_f^C/g_s) of a light (coloured) fermion f , i.e.

$$\frac{d_f}{e} = Q_f \frac{\alpha_{\text{em}}}{64\pi^3} \frac{R_f m_f}{M_a^2} \sum_{\tilde{f}=\tilde{t},\tilde{b},\tilde{\tau}} N_f^c \xi_{\tilde{f}} Q_{\tilde{f}}^2 \left[F\left(\frac{M_{\tilde{f}_1}^2}{M_a^2}\right) - F\left(\frac{M_{\tilde{f}_2}^2}{M_a^2}\right) \right], \quad (4.1)$$

$$\frac{d_f^C}{g_s} = \frac{\alpha_s}{128\pi^3} \frac{R_f m_f}{M_a^2} \sum_{\tilde{q}=\tilde{t},\tilde{b}} \xi_{\tilde{q}} \left[F\left(\frac{M_{\tilde{q}_1}^2}{M_a^2}\right) - F\left(\frac{M_{\tilde{q}_2}^2}{M_a^2}\right) \right], \quad (4.2)$$

where Q_f ($Q_{\tilde{f}}$) stands for the electric charge of a (scalar) fermion given in $|e|$ units, $N_{\tilde{f}}^c$ is the colour factor of the scalar fermion \tilde{f} ($N_{\tilde{\tau}}^c = 1$ and $N_{\tilde{t}}^c = N_{\tilde{b}}^c = 3$), $R_f = \cot\beta$ for the up-family fermions, $R_f = \tan\beta$ for the down-family ones. In addition, we have defined

$$\xi_{\tilde{f}} = -R_f \frac{\sin 2\theta_f m_f \text{Im}(\mu e^{i\delta_f})}{\sin\beta \cos\beta v^2}, \quad (4.3)$$

$$F(z) = \int_0^1 dx \frac{x(1-x)}{z-x(1-x)} \ln \left[\frac{x(1-x)}{z} \right]. \quad (4.4)$$

In Eq. (4.3), $\delta_f = \arg(A_f - R_{\tilde{f}}\mu^*)$ and θ_f indicates the mixing angle between weak and mass eigenstates of \tilde{f} . Since the off-diagonal elements of the scalar-quark and lepton mass matrices of the third generation may be larger than the difference of the diagonal entries, angles θ_f close to 45° are obtained in a natural way. Further discussion and more details of the calculation may be found in [25].

The present status of measurements of the electron and neutron EDMs is as follows [32]:

$$\left(\frac{d_e}{e}\right)_{\text{exp}} = (-0.27 \pm 0.83) \times 10^{-26} \text{ cm [33]}, \quad (4.5)$$

$$\left(\frac{d_e}{e}\right)_{\text{exp}} = (0.18 \pm 0.12 \pm 0.10) \times 10^{-26} \text{ cm [34]}, \quad (4.6)$$

$$\left(\frac{d_n}{e}\right)_{\text{exp}} = (0.26 \pm 0.40 \pm 0.16) \times 10^{-25} \text{ cm [35]}. \quad (4.7)$$

The experimental numbers listed here contain an amount of theoretical uncertainty originating from the model used for the heavy atoms, such as ^{105}Tl , or from the description of neutron's wave function in the heavy nucleus [36]. Notwithstanding the possible uncertainties in the determination of d_e , we should regard the 1σ upper bound, $|d_e/e| < 1.1 \times 10^{-26}$ cm, stated in Eq. (4.5) as a conservative one, when compared to the improved bound in Eq. (4.6). In particular, the 2σ upper bound on the electron EDM coming from the latter experimental analysis is $|d_e/e| < 0.5 \times 10^{-26}$ cm. Finally, the 1σ and 2σ upper bounds on the neutron EDM are $|d_n/e| < 0.69 \times 10^{-25}$ cm and $|d_n/e| < 1.12 \times 10^{-25}$ cm, respectively.

It is interesting to confront the theoretical predictions obtained for d_e/e and d_n/e in the MSSM with the corresponding experimental bounds mentioned above. In Table 1, we present numerical estimates for the case $|A| = |A_t| = |A_b| = |A_\tau| = 1$ TeV, $\arg(A) = 90^\circ$ and $M_a = 150$ GeV, while the kinematic parameters $\tan\beta$, μ , M_{SUSY} have been varied discretely. We should note that the largest contribution to the neutron EDM comes from

$\tan \beta$	M_{SUSY} [TeV]	$ d_e/e $ [10 ⁻²⁷ cm]			$ d_n/e $ [10 ⁻²⁶ cm]		
		$\mu = 0.5,$	1,	2 TeV	$\mu = 0.5,$	1,	2 TeV
2	0.5	0.7	1.6	5.9	0.7	1.5	5.6
	0.6	0.3	0.7	1.6	0.3	0.7	1.5
	0.7	0.2	0.4	0.8	0.2	0.4	0.8
4	0.5	1.2	2.5	5.5	1.1	2.2	4.9
	0.6	0.6	1.1	2.3	0.5	1.0	2.1
	0.7	0.3	0.6	1.3	0.3	0.6	1.2
10	0.5	2.9	5.8	12.	2.6	5.2	11.
	0.6	1.3	2.7	5.4	1.2	2.4	4.8
	0.7	0.7	1.5	3.0	0.7	1.3	2.7
20	0.5	6.0	12.	24.	5.5	11.	22.
	0.6	2.8	5.5	11.	2.6	5.1	10.
	0.7	1.5	3.1	6.2	1.4	2.9	5.7

Table 1: Numerical predictions for the electron and neutron EDMs in the MSSM, using $|A| = |A_t| = |A_b| = |A_\tau| = 1$ TeV, $\arg(A) = 90^\circ$ and $M_a = 150$ GeV ($m_b(M_Z) = 3$ GeV).

the CEDM of the d quark. Furthermore, scalar-top quarks have the biggest quantum effect on the e and n EDMs for $2 \lesssim \tan \beta \lesssim 30$. Taking the numerical estimates in Table 1 into account, we shall consider the following three representative scenarios:

$$\begin{aligned}
\text{I.} \quad & M_{\text{SUSY}} = 0.5 \text{ TeV}, \quad |A| = 1 \text{ TeV}, \quad \mu = 2 \text{ TeV}, \quad \tan \beta = 2, \\
\text{II.} \quad & M_{\text{SUSY}} = 0.5 \text{ TeV}, \quad |A| = 1 \text{ TeV}, \quad \mu = 2 \text{ TeV}, \quad \tan \beta = 4, \\
\text{III.} \quad & M_{\text{SUSY}} = 0.5 \text{ TeV}, \quad |A| = 1 \text{ TeV}, \quad \mu = 1 \text{ TeV}, \quad \tan \beta = 20. \quad (4.8)
\end{aligned}$$

In the next section, we shall analyze the phenomenological consequences of the scenarios given by Eq. (4.8) on the currently operating and future high-energy colliders.

5 Phenomenological implications for Higgs searches

We shall discuss the main phenomenological consequences of CP violation in the Higgs sector of the MSSM on the Higgs-boson mass spectrum and on the production cross sections of the lightest Higgs boson H_1 . In general, CP violation modifies the couplings of the Higgs particles to fermions and to the W and Z bosons, as well as their self-interactions. Furthermore, quadrilinear interactions involving Higgs bosons change as well, when CP-violating

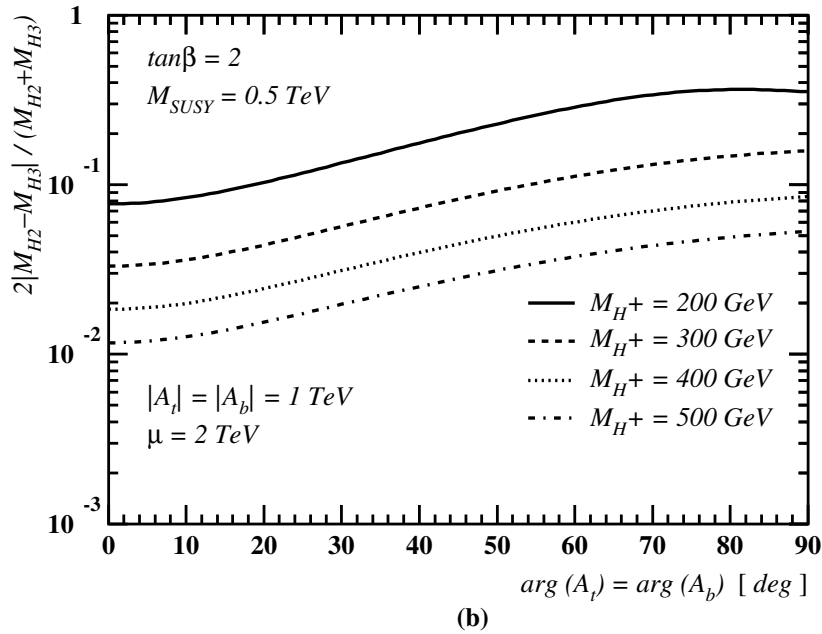
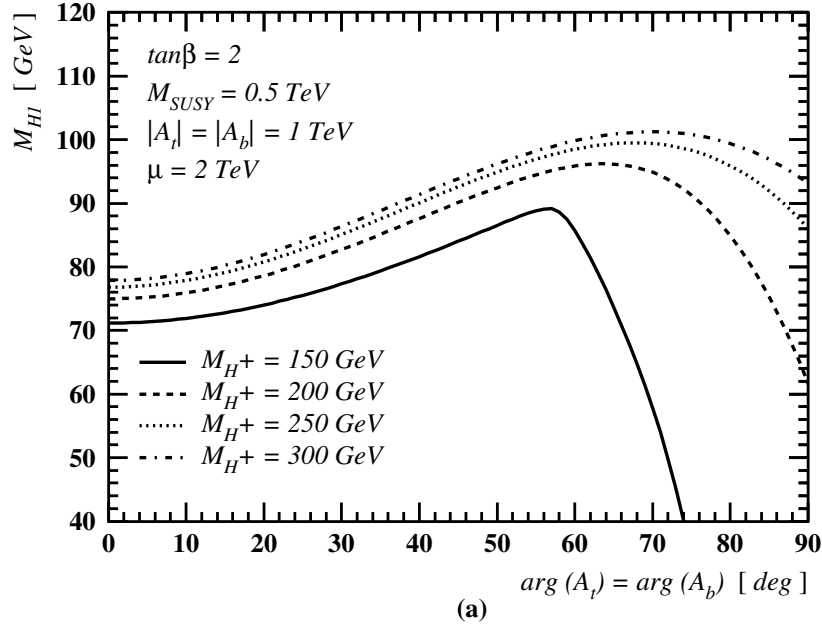
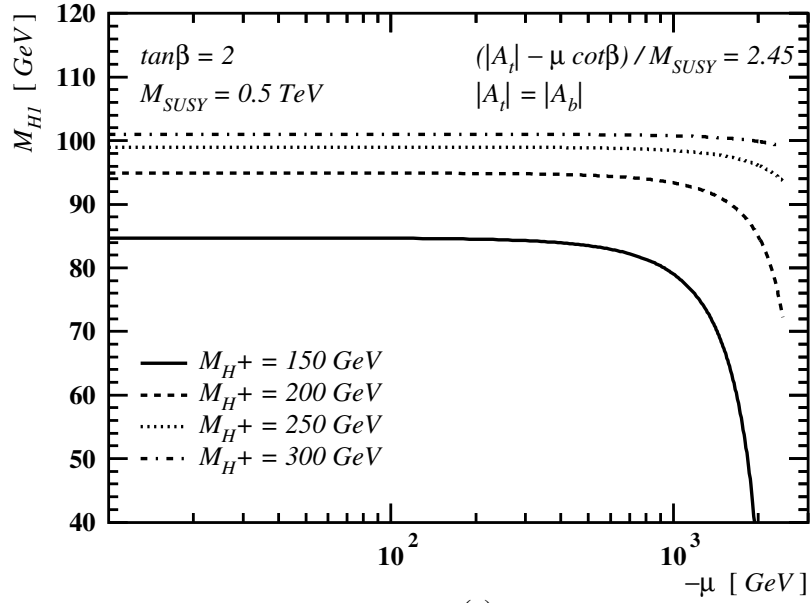
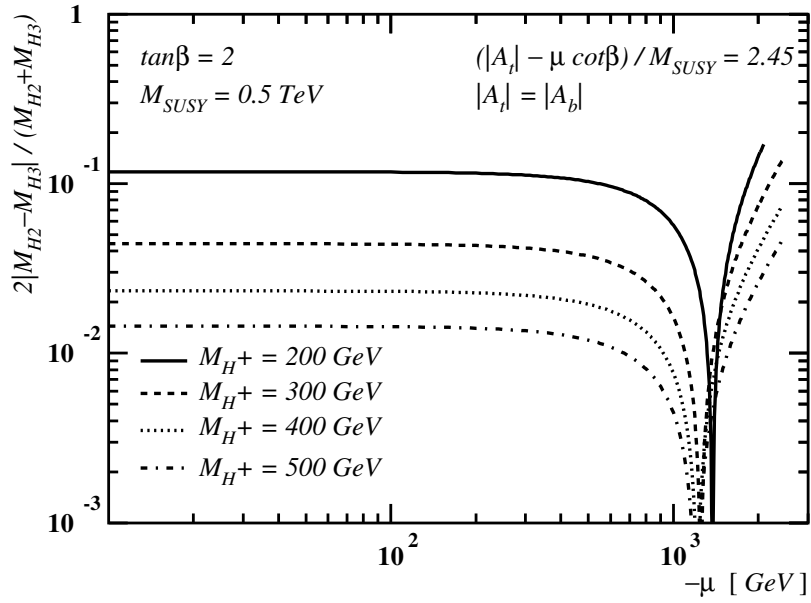


Figure 2: Numerical estimates of (a) M_{H_1} and (b) $2|M_{H_2} - M_{H_3}|/(M_{H_2} + M_{H_3})$ as a function of the CP-violating phase $\arg(A_t)$.



(a)



(b)

Figure 3: Numerical estimates of (a) M_{H1} and (b) $2|M_{H2} - M_{H3}| / (M_{H2} + M_{H3})$ as a function of μ in the CP-conserving MSSM.

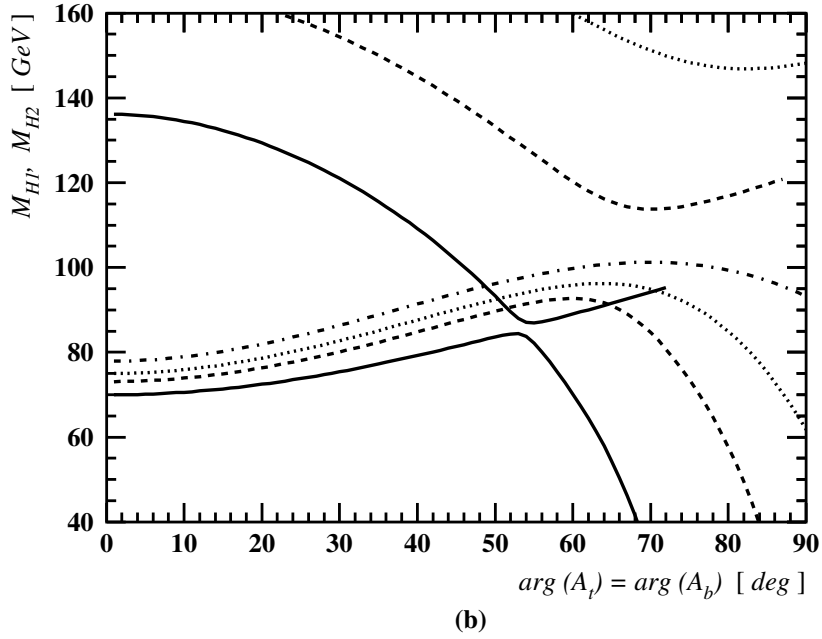
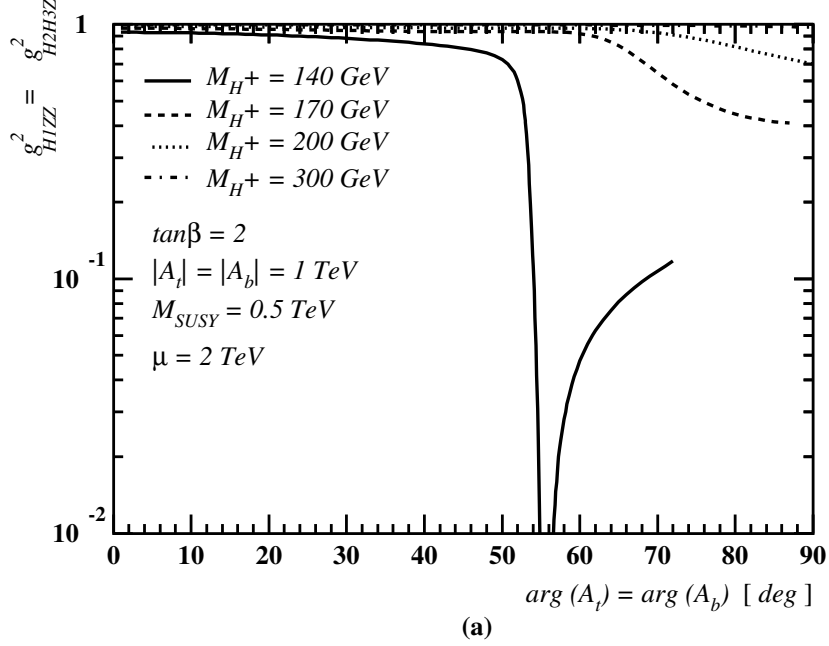


Figure 4: Numerical predictions for (a) $g_{H_1ZZ}^2 = g_{H_2H_3Z}^2$ and (b) $M_{H_1} \leq M_{H_2}$ as a function of $\arg(A_t)$. The definitions of g_{H_1ZZ} and $g_{H_2H_3Z}$ are given in Eqs. (5.6) and (5.7), respectively.

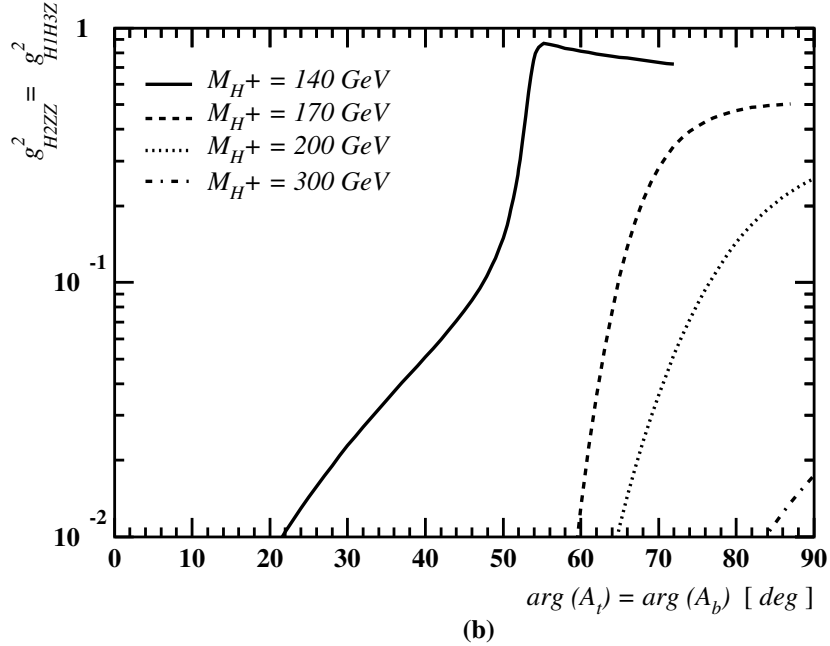
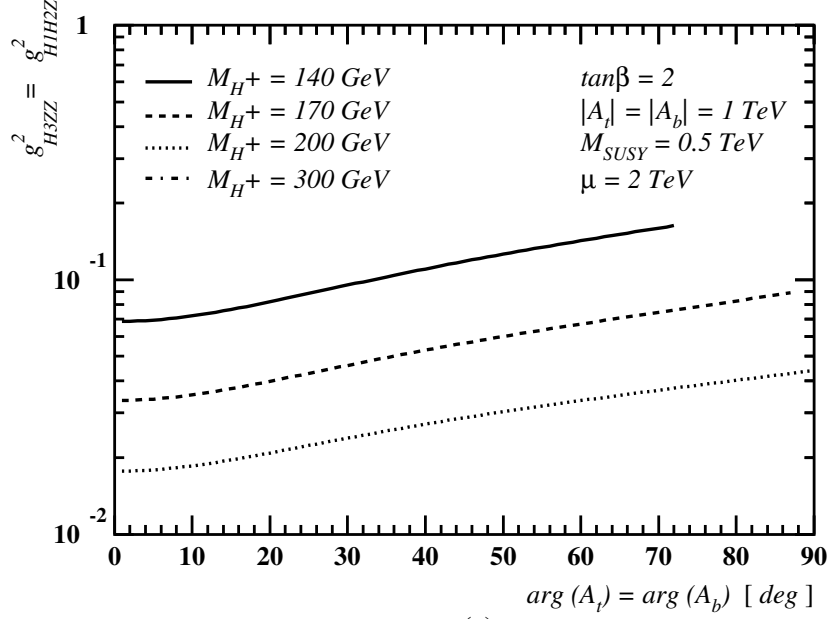


Figure 5: Numerical predictions for (a) $g_{H_3ZZ}^2 = g_{H_1H_2Z}^2$ and (b) $g_{H_2ZZ}^2 = g_{H_1H_3Z}^2$ as a function of $\arg(A_t)$. The definition of g_{H_1ZZ} and $g_{H_2H_3Z}$ are given in Eqs. (5.6) and (5.7), respectively.

effects due to a mixing of Higgs states are included. However, the latter interactions as well as the trilinear Higgs self-couplings are generally sub-dominant in production processes, and hence we should not consider these here.

At the high-energy machines LEP2 and Tevatron, the dominant production mechanism of the lightest Higgs boson is the Bjorken process in association with W and Z bosons [37,38], e.g. $e^+e^- \rightarrow H_1 Z$ or the partonic process $u\bar{d} \rightarrow W^+ H_1$. Such reactions involve the couplings of Higgs bosons to W and Z bosons. In the presence of CP violation, these couplings may be read off by the Lagrangians

$$\mathcal{L}_{HVV} = g_w M_W (c_\beta O_{2i} + s_\beta O_{3i}) \left(H_{(4-i)} W_\mu^+ W^{-,\mu} + \frac{1}{2c_w^2} H_{(4-i)} Z_\mu Z^\mu \right), \quad (5.1)$$

$$\mathcal{L}_{HH^\pm W^\mp} = \frac{g_w}{2} (c_\beta O_{3i} - s_\beta O_{2i} + i O_{1i}) W^{+,\mu} (H_{(4-i)} \overleftrightarrow{\partial}_\mu H^-) + \text{H.c.}, \quad (5.2)$$

$$\begin{aligned} \mathcal{L}_{HHZ} &= \frac{g_w}{4c_w} \left[O_{1i} (c_\beta O_{3j} - s_\beta O_{2j}) - O_{1j} (c_\beta O_{3i} - s_\beta O_{2i}) \right] \\ &\quad \times Z^\mu (H_{(4-i)} \overleftrightarrow{\partial}_\mu H_{(4-j)}), \end{aligned} \quad (5.3)$$

where $c_w = M_W/M_Z$ and $\overleftrightarrow{\partial}_\mu \equiv \overrightarrow{\partial}_\mu - \overleftarrow{\partial}_\mu$. Note that the Z boson can only couple to two different Higgs particles as stated in the Lagrangian (5.3). The reason is that Bose symmetry forbids any antisymmetric derivative coupling of a vector particle to two identical real scalar fields.

Making now use of the following identity, which governs the matrix elements of O (assuming $\det O = 1$):

$$O_{lk} = \frac{1}{2} \sum_{n,m,i,j=1}^3 \varepsilon_{nml} \varepsilon_{ijk} O_{ni} O_{mj}, \quad (5.4)$$

it is not difficult to derive an important relation between the couplings of the neutral Higgs bosons to the gauge bosons, namely

$$g_{H_k VV} = \varepsilon_{ijk} g_{H_i H_j Z}, \quad (5.5)$$

where $g_{H_i VV}$ ($V = W^\pm, Z$) are the Higgs-gauge-boson couplings normalized to the SM value, i.e.

$$g_{H_i VV} = c_\beta O_{2i} + s_\beta O_{3i}, \quad (5.6)$$

while $g_{H_i H_j Z}$ is defined by the expression between the brackets in Eq. (5.3),

$$g_{H_i H_j Z} = O_{1i} (c_\beta O_{3j} - s_\beta O_{2j}) - O_{1j} (c_\beta O_{3i} - s_\beta O_{2i}). \quad (5.7)$$

From the relation (5.5) and the unitarity constraint

$$\sum_{i=1}^3 g_{H_i Z Z}^2 = 1, \quad (5.8)$$

the immediate result is that the knowledge of two $g_{H_i ZZ}$ is sufficient to determine the whole set of couplings of the neutral Higgs to the gauge bosons [39].

The essential difference between a CP-conserving MSSM Higgs sector and a CP-violating one is that mixing effects between the would-be CP-odd and CP-even Higgs bosons are present in the latter case. Such scalar–pseudoscalar mixing effects are induced by radiative corrections to the Higgs potential [9]. The characteristic size of the CP-violating off-diagonal terms in the Higgs-boson mass matrix may be estimated by

$$M_{SP}^2 \simeq \mathcal{O} \left(\frac{m_t^4}{v^2} \frac{|\mu||A_t|}{32\pi^2 M_{\text{SUSY}}^2} \right) \sin \phi_{\text{CP}} \times \left(6, \frac{|A_t|^2}{M_{\text{SUSY}}^2}, \frac{|\mu|^2}{\tan \beta M_{\text{SUSY}}^2}, \frac{\sin 2\phi_{\text{CP}}}{\sin \phi_{\text{CP}}} \frac{|\mu||A_t|}{M_{\text{SUSY}}^2} \right), \quad (5.9)$$

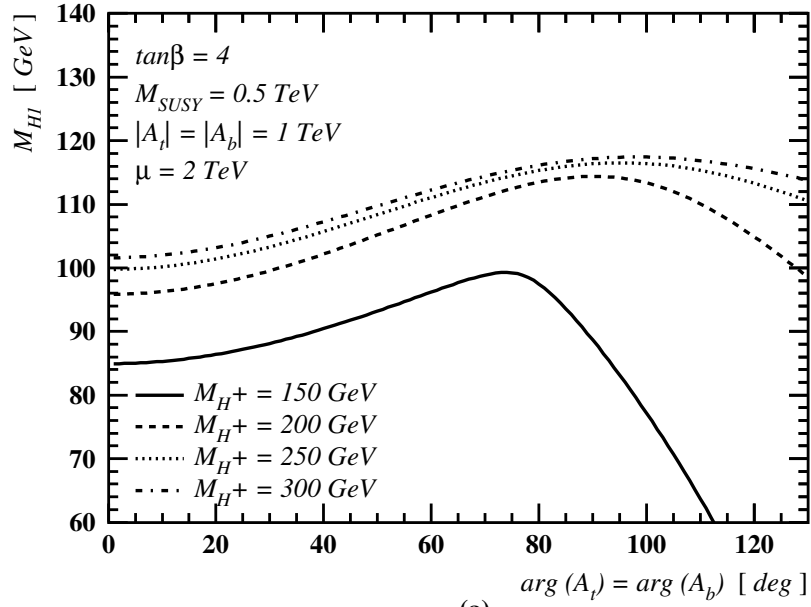
where the last bracket summarizes the relative size of the different contributions, and

$$\phi_{\text{CP}} = \arg(A_t \mu) + \xi. \quad (5.10)$$

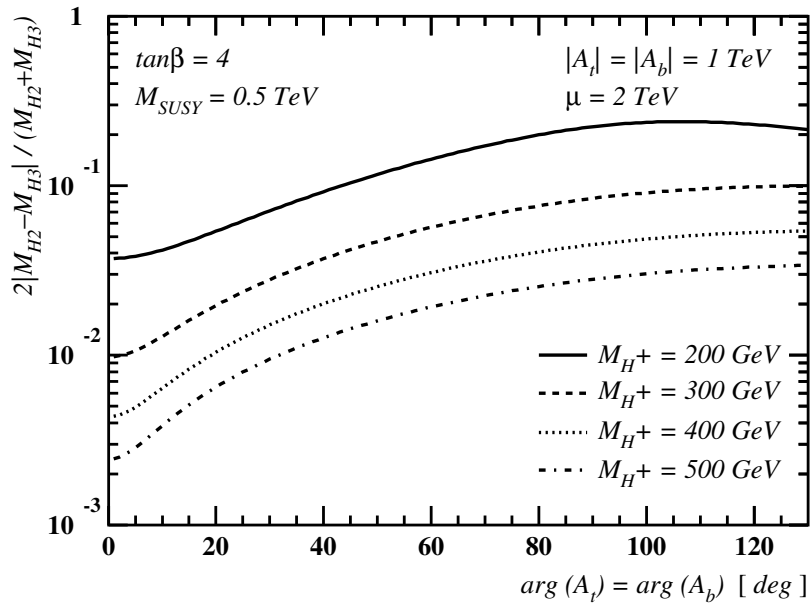
For $|\mu|$ and $|A_t|$ values larger than the arithmetic average of the scalar-top-quark masses squared, denoted as M_{SUSY} (cf. Eq. (A.16)), the CP-violating effects can be significant. For instance, if $|\mu| \simeq |A_t| \simeq 2M_{\text{SUSY}}$, and $\phi_{\text{CP}} \simeq 90^\circ$, the off-diagonal terms of the neutral Higgs-boson mass matrix may be of the order of $(100 \text{ GeV})^2$. These potentially large mixing effects have important consequences, since they lead to drastic variations in the definition of the neutral Higgs-boson masses and in the couplings of the Higgs states to the gauge bosons. Because of the quantum nature of the CP-violating mixing effects and the known decoupling property of heavy states in the loop in SUSY theories, the phenomenology of the lightest Higgs boson will only be important for low values of M_{H^+} . For the same reason, M_{H^+} values much larger than the electroweak scale lead to predictions for the mass of the lightest Higgs boson H_1 and for the couplings of the H_1 scalar to the gauge bosons which are equivalent to those obtained in the CP-invariant theory. The only difference in the CP-violating case is that the relevant scalar-top mixing parameter entering the definition of M_{H_1} is now given by

$$|\tilde{A}_t| = |A_t - \mu^* / \tan \beta|. \quad (5.11)$$

In addition to the effects induced by scalar-top quarks, Yukawa interactions due to scalar-bottom quarks can also be significant for large values of $\tan \beta$, so as to lead to sizeable contributions to the elements of the Higgs-boson mass-matrix. As was discussed in Section 4, however, the contributions of the scalar-bottom sector are limited by constraints that originate from the electron and neutron EDMs. In general, unless cancellations occur between different contributions to the EDMs, the CP-violating quantum effects coming from the scalar-bottom sector are expected to be small.

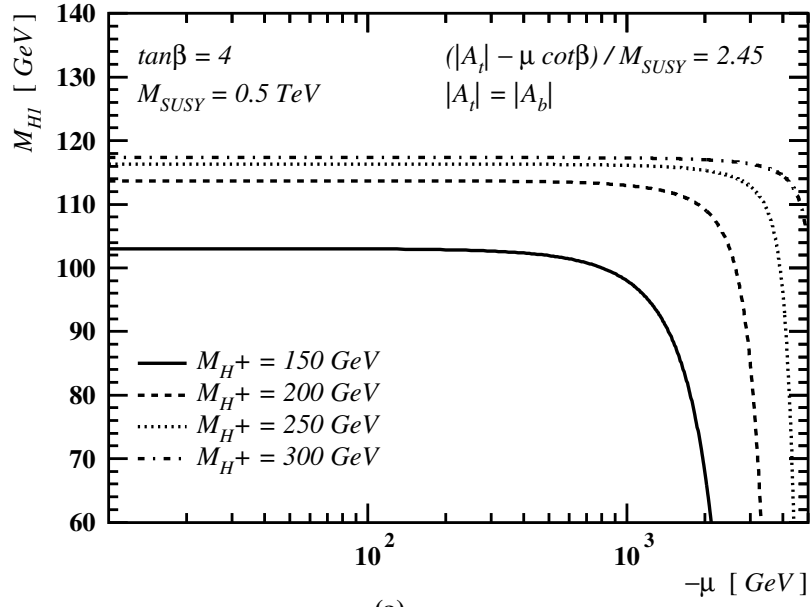


(a)

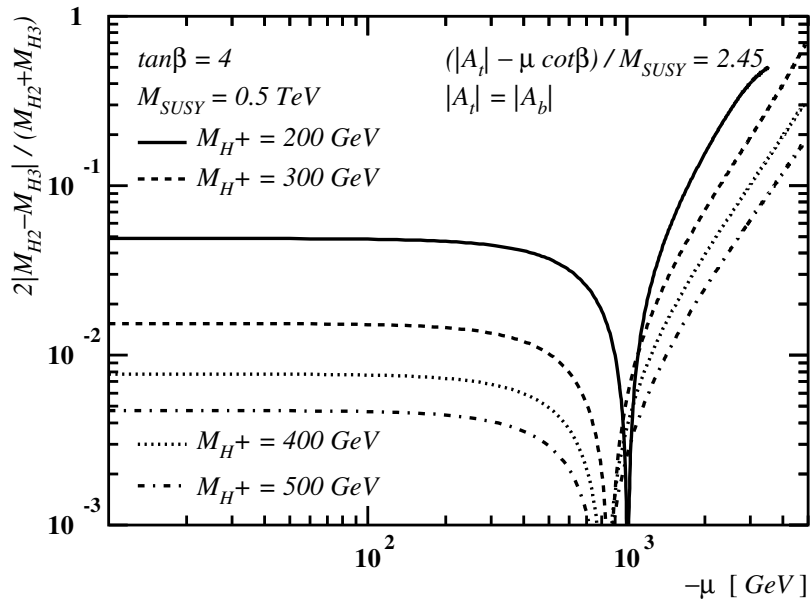


(b)

Figure 6: The same as in Fig. 2, but with $\tan\beta = 4$.

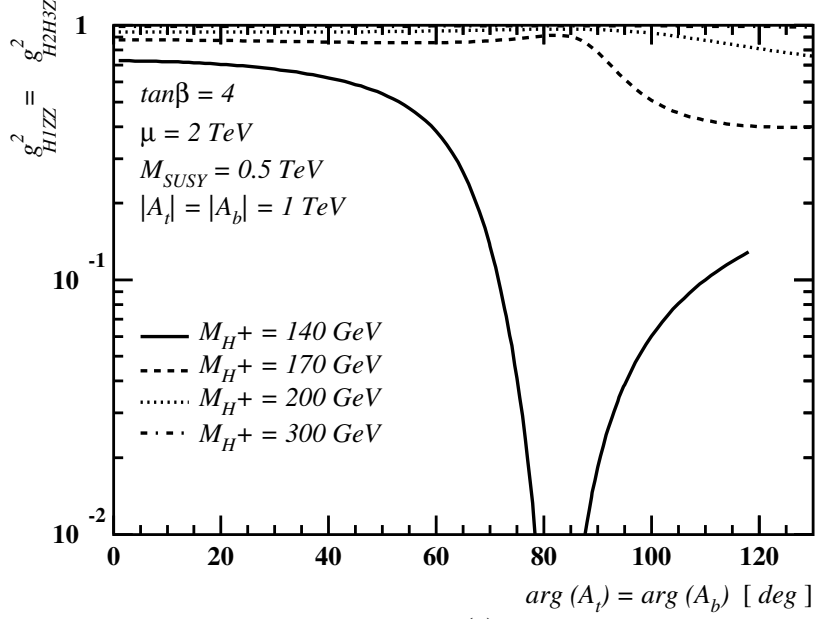


(a)

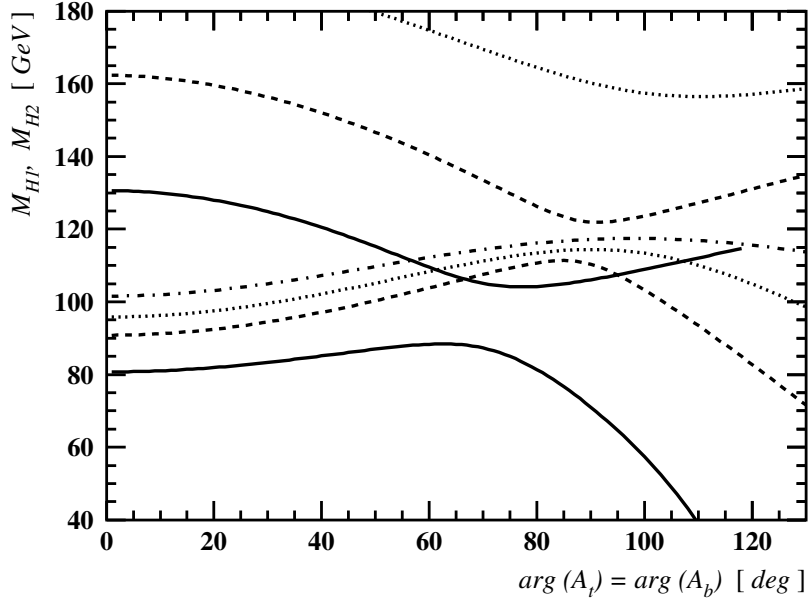


(b)

Figure 7: The same as in Fig. 3, but with $\tan\beta = 4$.



(a)



(b)

Figure 8: The same as in Fig. 4, but with $\tan\beta = 4$.

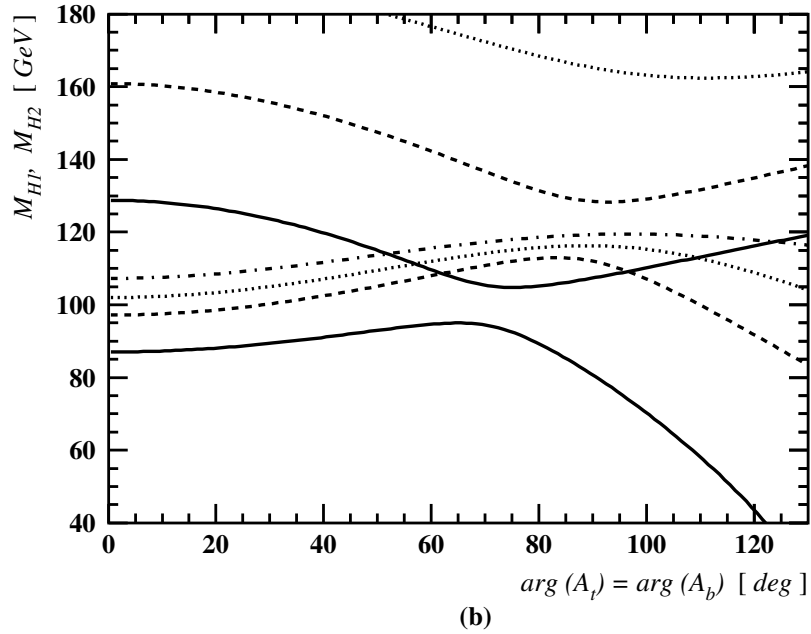
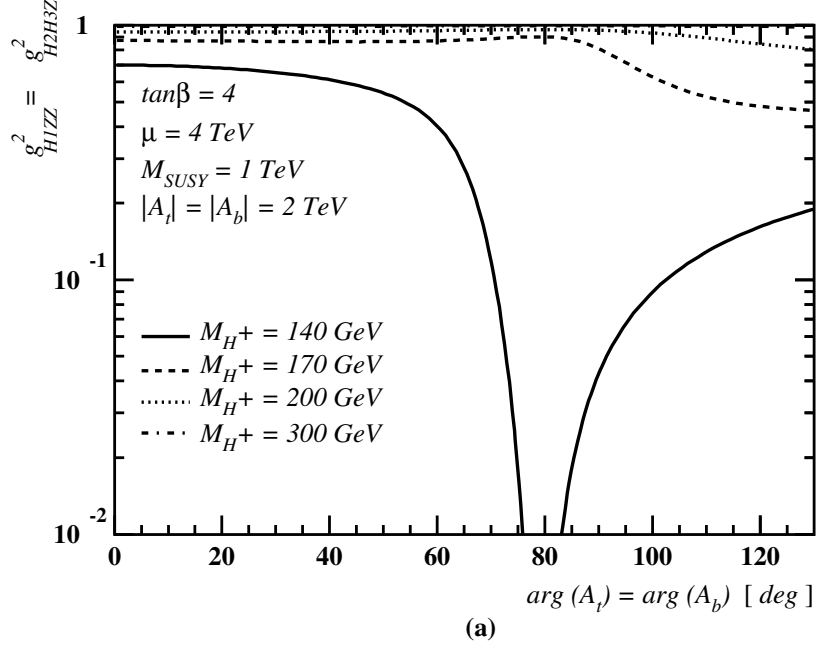


Figure 9: The same as in Fig. 8, but setting $M_{SUSY} = 1 \text{ TeV}$, $|A_t| = |A_b| = 2 \text{ TeV}$ and $\mu = 4 \text{ TeV}$.

In Fig. 2, we present numerical estimates of the lightest Higgs-boson mass M_{H_1} and of the relative mass splitting of the two heaviest Higgs bosons, H_2 and H_3 , as a function of $\phi_{\text{CP}} \equiv \arg(A_t)$, for different values of the charged Higgs-boson mass and for $\tan\beta = 2$, $M_{\text{SUSY}} = 0.5 \text{ TeV}$, $|A_t| = 1 \text{ TeV}$ and $\mu = 2 \text{ TeV}$. We must remark that relatively large values of the $|\mu|$ and $|A_t|$ parameters have been chosen, in order to make the CP-violating effects relevant. In fact, for these values of the trilinear couplings, we are at the edge of the limit of validity of the expansion we used to compute the expression of the quartic couplings in the RG-improved Higgs potential (see appendix). However, we may verify that the neglected terms would lead to a slight increase of the CP-violation effects we have computed. For the region of parameters we are considering, the omitted terms are of the order of finite two-loop corrections to the effective potential, which are not included in the analytic expression of the one-loop RG-improved effective potential. Moreover, if all SUSY-mass parameters are rescaled by a factor 2, the validity of the expansion improves dramatically, while the physical results are only slightly modified. Later on, we shall explicitly demonstrate this point by giving a specific example (cf. Fig. 9). In this context, we believe that our results should be regarded as conservative estimates of the possible size of the CP-violating effects in the Higgs sector.

In Fig. 2, the dependence of M_{H_1} on $\arg(A_t)$ may be understood as follows: if the moduli of the parameters A_t and μ are kept fixed, the mass of the lightest neutral Higgs boson H_1 starts increasing, as a function of $\arg(A_t)$, up to a maximum; it then decreases rapidly. This kinematic dependence may be attributed to the fact that the modulus of the scalar-top mixing parameter \tilde{A}_t increases monotonically for the range $0 \leq \arg(A_t) \leq 180^\circ$. We find that the behaviour of M_{H_1} as a function of $\arg(A_t)$ is very analogous to the one that would have been obtained for the lightest CP-even Higgs boson in the CP-invariant theory if we had varied $|\tilde{A}_t|$ given in Eq. (5.11). However, unlike the CP-conserving case, the effects of the Higgs-sector CP violation can give rise to much larger mass splittings between the two heaviest Higgs bosons H_2 and H_3 as a function of $\arg(A_t)$ [9]. This fact is difficult to infer from the kinematic dependence of M_{H_1} alone. In Fig. 2(b), we see that even in the case of $M_{H^+} = 200 \text{ GeV}$, the CP-violating effects may lead to a relative mass splitting of the two heaviest neutral Higgs bosons of the order of 30%.

In order to get an idea of how much of the above effects are due to the presence of CP violation, we plot in Fig. 3 the behaviour of the same neutral Higgs-boson masses as a function of the parameter μ , where $\phi_{\text{CP}} = 0$ is considered and the scalar-top mixing parameter $|\tilde{A}_t|$ is fixed to the value that yields the maximum for the lightest CP-even Higgs-boson mass M_h for large values of M_{H^+} . Figure 3 exhibits the dependence of $M_h \equiv M_{H_1}$ as a function of μ . We find that large values of μ tend to reduce M_h and increase the degree

of the mass splitting between the heaviest CP-even Higgs boson and the CP-odd Higgs scalar, $2|M_{H_2} - M_{H_3}|/(M_{H_2} + M_{H_3})$. In particular, we observe that for the same value of M_{H_1} , $2|M_{H_2} - M_{H_3}|/(M_{H_2} + M_{H_3})$ is much smaller in the CP-invariant theory than in the CP-violating one.

It is worth investigating whether the CP-violating Higgs effects could lead to not-yet-explored open windows in the parameter space of the theory that cannot be accessed by the running experiments and are not present in the CP-conserving case. To this end, we plot in Figs. 4 and 5 the Higgs–gauge-boson couplings as a function of $\arg(A_t)$, for the same choice of SUSY parameters as those in Fig. 2. For low values of M_{H^+} , the Higgs boson that couples predominantly to the Z boson is H_1 (H_2). For $M_{H^+} = 140$ GeV, there is an interesting region of parameters for which the H_1ZZ coupling becomes small, rendering the detection of the H_1 boson via the H_1ZZ channel at LEP2 difficult. However, in the same region of parameters, the mass of the next-to-lightest neutral Higgs state, H_2 , is smaller than 95 GeV and the H_2ZZ coupling becomes large. Therefore, in this particular kinematic range of parameters, the H_2ZZ channel is the only relevant one that helps to exclude these small values of $\tan\beta$ and charged Higgs-boson masses at LEP2. For larger values of M_{H^+} , the situation resembles more the CP-invariant theory. Even for $M_{H^+} = 170$ GeV, the suppression of the H_1ZZ coupling is not sufficiently large to produce a significant change in the present LEP2 bound. Therefore, very analogously to the CP-conserving case [8], only a small region of parameters, for which the lightest CP-even Higgs boson is heavy enough, is still experimentally allowed, i.e. for large values of the scalar-top mixing mass parameter $|\tilde{A}_t|$ ($\arg(A_t) \simeq 60^\circ\text{--}90^\circ$) and for relatively large values of the charged Higgs-boson mass.

More interesting is the situation at intermediate values of $\tan\beta$. Even though, as displayed in Figs. 6 and 7, the dependence of the Higgs masses on the CP-violating phases and the scalar-top mixing parameters is similar to the one obtained for $\tan\beta = 2$, the region for which the coupling of the lightest neutral Higgs boson to the gauge bosons becomes small now displays larger values of the H_1 and H_2 masses. In this range of kinematic parameters, the experimental detection of the H_1 and H_2 particles becomes more difficult at LEP2. In Table 2, we present the current reach of LEP2 for the H_1 -boson mass as a function of g_{H_1ZZ} , and independently, for (M_{H_1}, M_{H_2}) versus $g_{H_1H_2Z}$, assuming $M_{H_1} \approx M_{H_2}$. As can then be seen from Fig. 8 for the case of a relatively light charged Higgs scalar $M_{H^+} = 140$ GeV, we get regions for which the lightest Higgs-boson mass M_{H_1} is as small as 60–70 GeV and the H_1ZZ coupling is small enough for the H_1 boson to escape detection at the latest LEP2 run, with $\sqrt{s} = 189$ GeV. Moreover, the H_2 boson is too heavy to be detected through the H_2ZZ channel. In addition, either the coupling H_1H_2Z is too small or H_2 is too heavy to allow the Higgs detection in the H_1H_2Z channel (see also Fig. 10). To

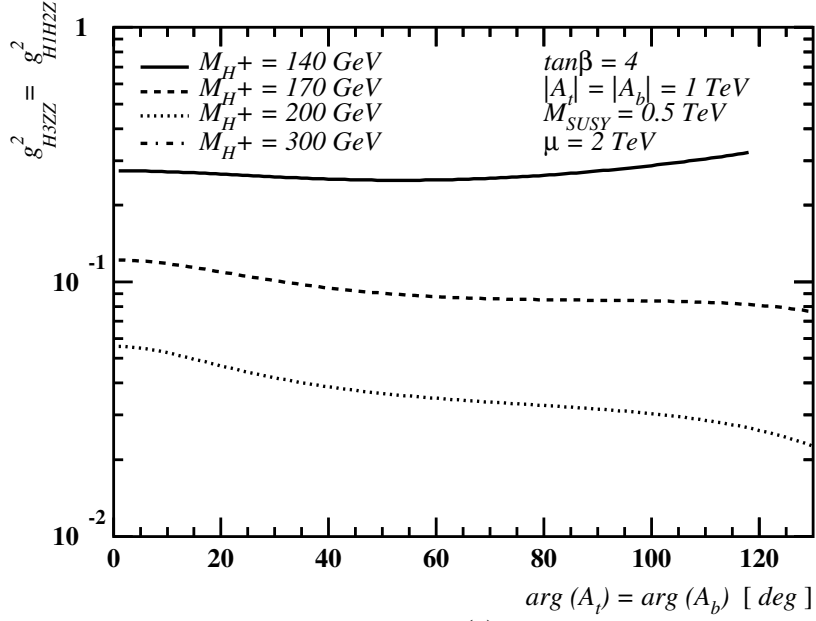
$g_{H_1 ZZ}^2$	M_{H_1} [GeV]	$g_{H_1 H_2 Z}^2$	$M_{H_1} \approx M_{H_2}$ [GeV]
1	97	1	86
0.6	96	0.9	85
0.5	95	0.8	84
0.4	93	0.7	83
0.3	92	0.6	82
0.2	88	0.5	80
0.1	77	0.4	77
0.08	70	0.3	72

Table 2: Present experimental sensitivity of the couplings $g_{H_1 ZZ}^2$ and $g_{H_1 H_2 Z}^2$ as a function of M_{H_1} , assuming $M_{H_1} \approx M_{H_2}$. The results are obtained from four experiments combined at LEP2 with $\sqrt{s} = 189$ GeV.

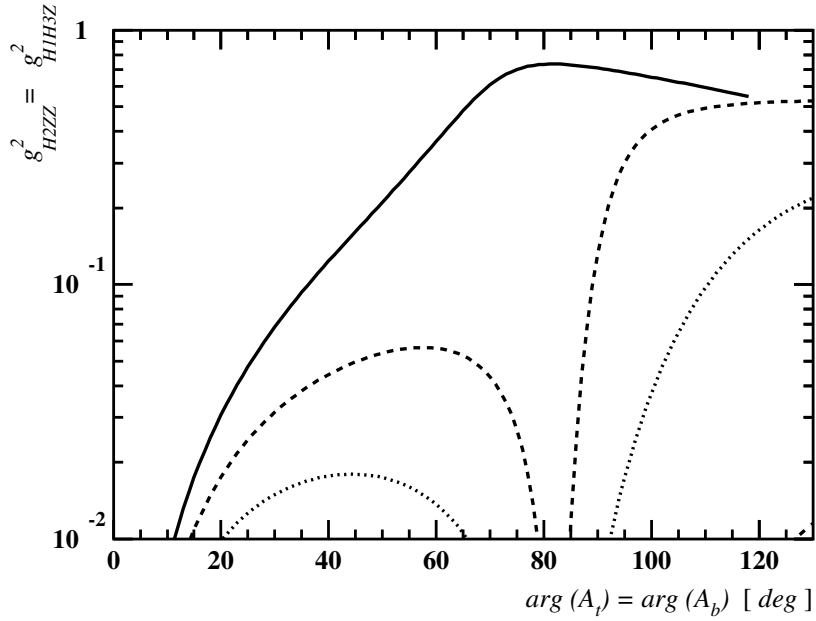
better gauge the validity of the expansion that has been used for the quartic couplings in the effective Higgs potential (see also the discussion in the appendix), we have plotted in Fig. 9 the same $\tan\beta$ scenario but rescaling M_{SUSY} , $|A_t| = |A_b|$ and μ by a factor of 2, i.e. $M_{\text{SUSY}} = 1$ TeV, $|A_t| = |A_b| = 2$ TeV and $\mu = 4$ TeV. We then find that M_{H_1} has only slightly increased and the kinematic dependence of the $H_1 ZZ$ coupling on the CP-violating phase $\arg(A_t)$ remained almost unchanged when compared to Fig. 8.

For very large values of $\tan\beta$, the CP-violating effects in the Higgs sector are constrained by the bounds on the EDM of the electron and neutron discussed in Section 4. If no cancellation mechanism is assumed to occur between the different EDM contributions, the CP-violating effects in the Higgs sector are then relatively small, and the phenomenological properties of the Higgs bosons become very similar to those obtained in the CP-invariant case. This feature is shown in Figs. 11–14, for the same quantities as those considered in Figs. 2–5. Notice that the actual bound on $\tan\beta$ coming from EDM constraints strongly depends on the exact value of the CP-odd phase, which we choose to be equal to 90° . In the high- $\tan\beta$ regime, the running b -quark mass m_b plays a central role. As we will see later on, m_b turns out to be a model-dependent quantity in the MSSM. So as to make definite predictions, however, we have set $m_b(\overline{m}_t) = 3$ GeV, where \overline{m}_t is the top-quark pole mass (cf. Eq. (A.12)).

It is now interesting to discuss whether the Tevatron collider together with its future upgraded facilities have the potential capabilities of exploring the open windows that are



(a)



(b)

Figure 10: The same as in Fig. 5, but with $\tan\beta = 4$.

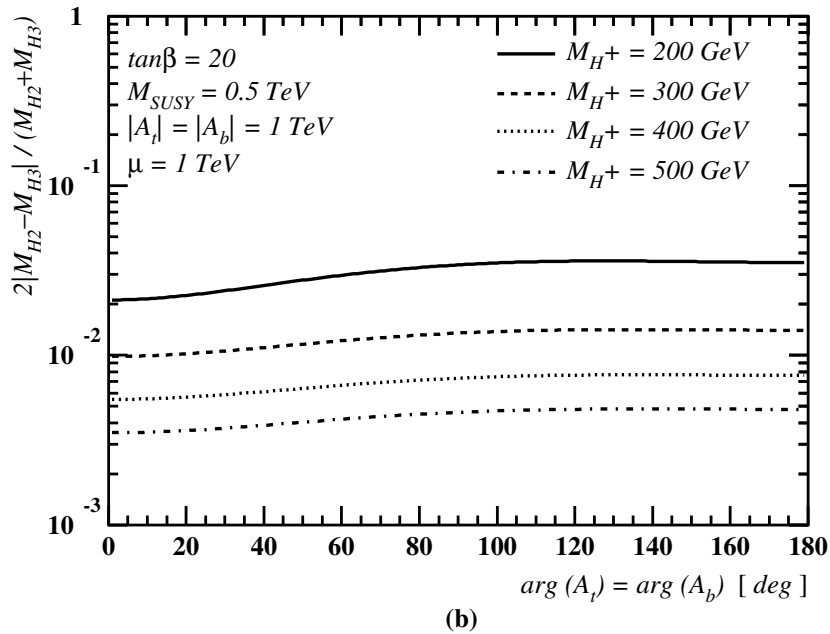
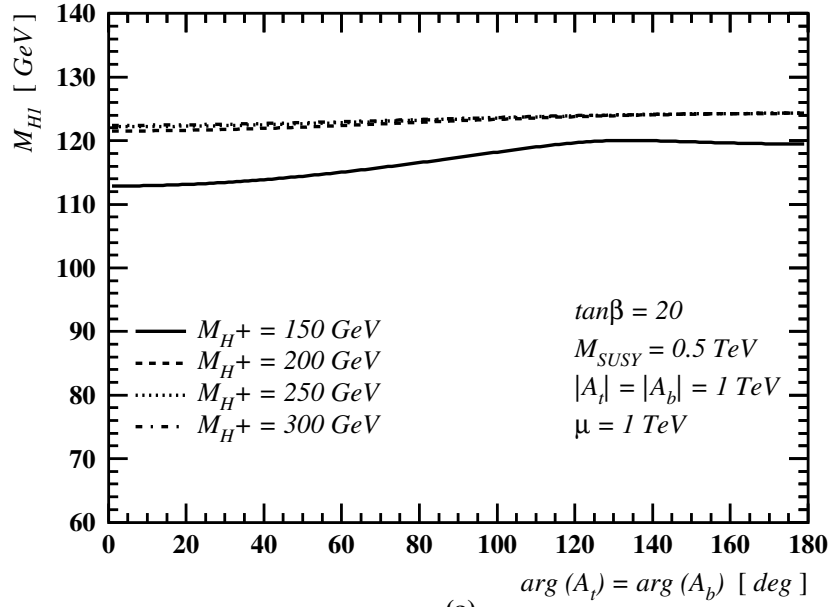
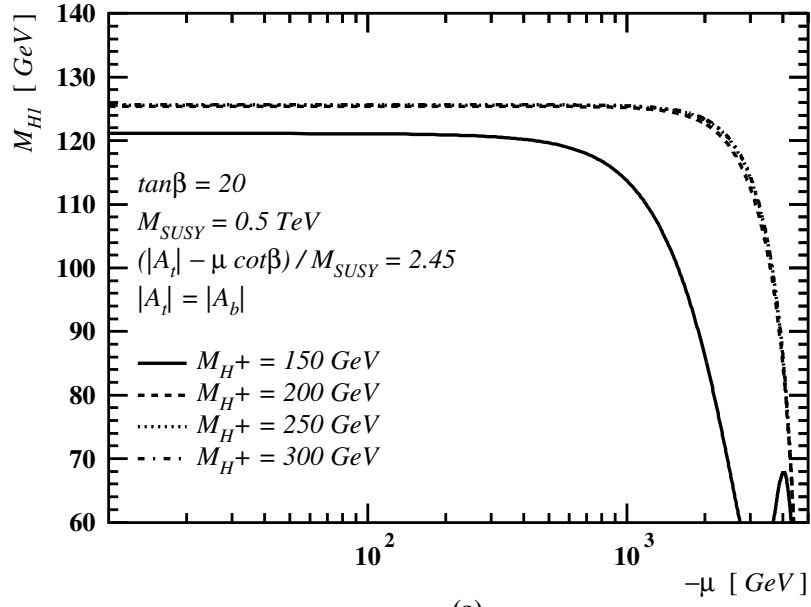
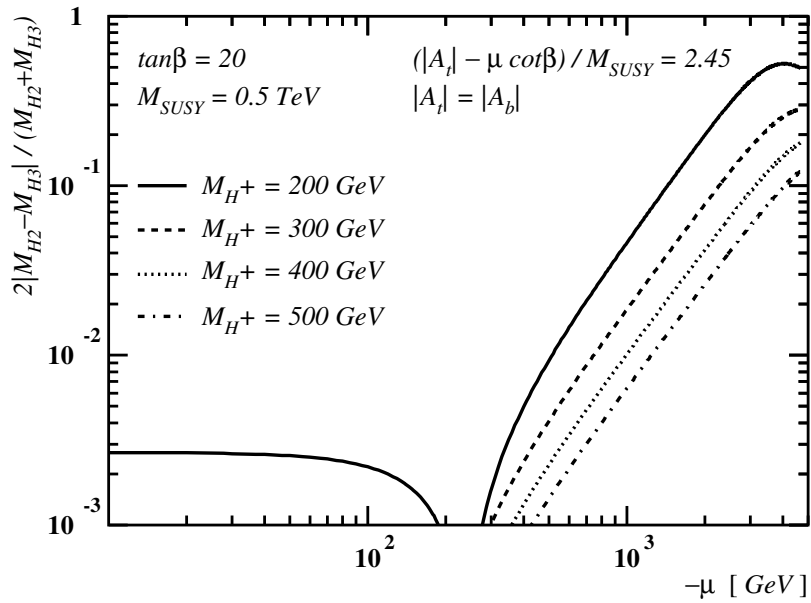


Figure 11: The same as in Fig. 2, but with $\tan\beta = 20$ and $\mu = 1$ TeV.

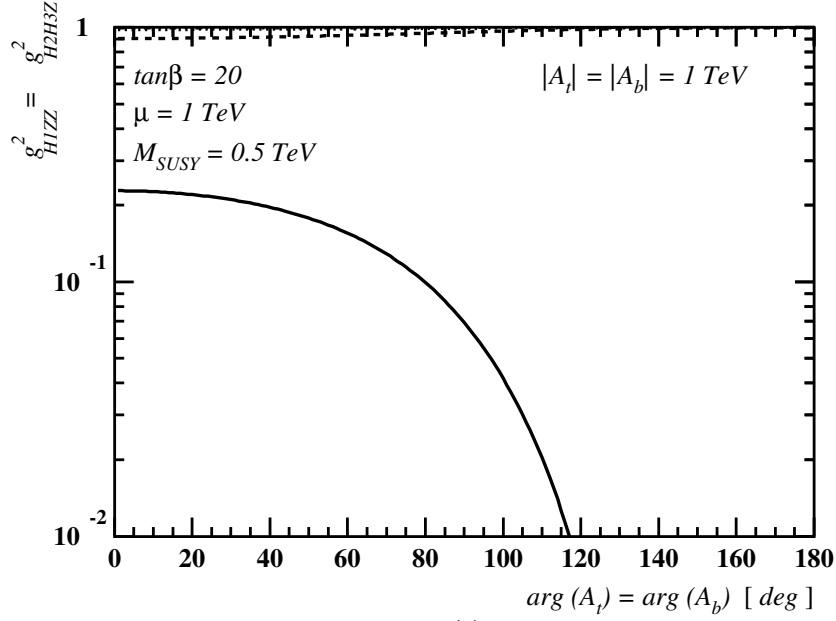


(a)

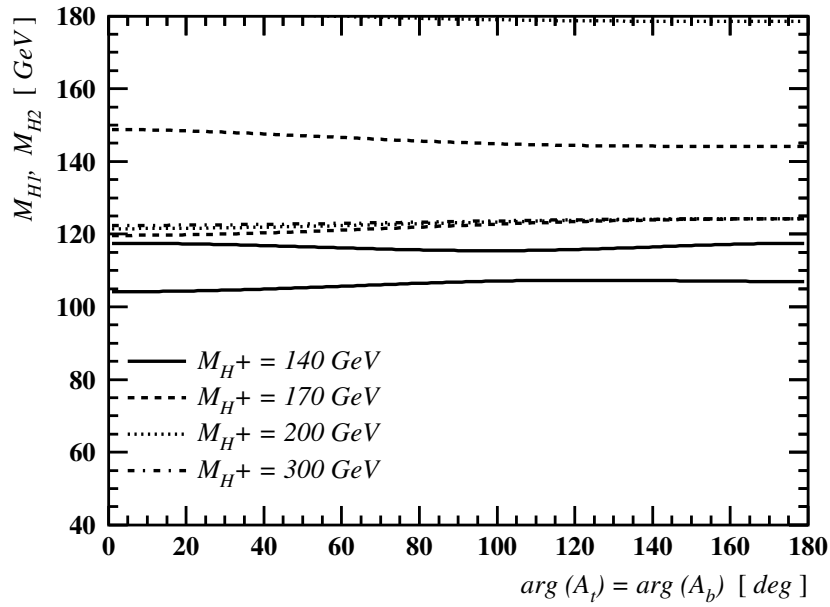


(b)

Figure 12: The same as in Fig. 3, but with $\tan\beta = 20$ and $\mu = 1$ TeV.

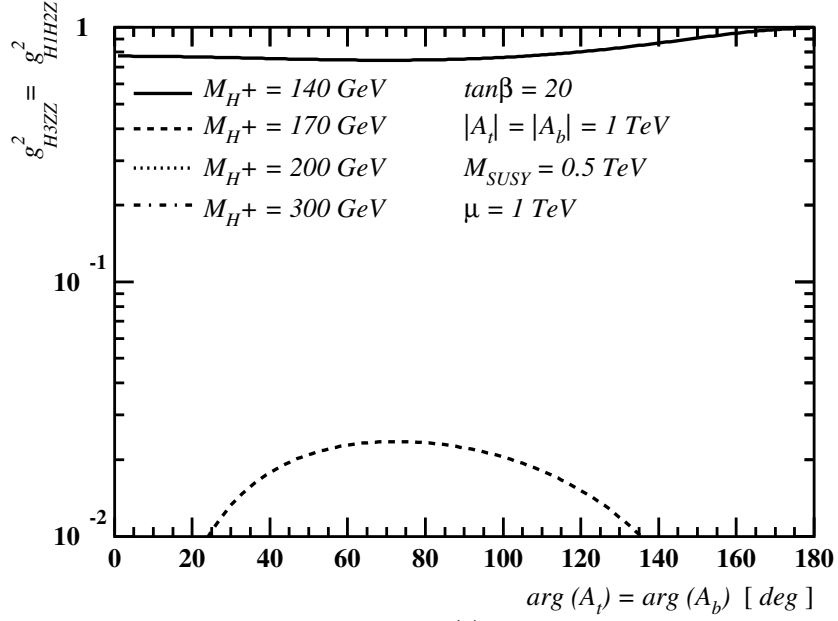


(a)

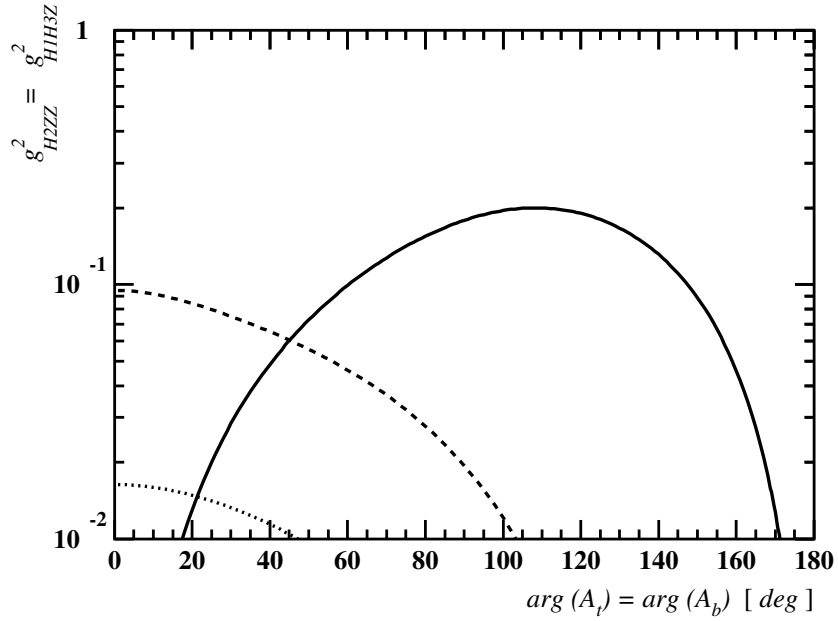


(b)

Figure 13: The same as in Fig. 4, but with $\tan\beta = 20$ and $\mu = 1 \text{ TeV}$.



(a)



(b)

Figure 14: The same as in Fig. 5, but with $\tan\beta = 20$ and $\mu = 1 \text{ TeV}$.

not accessible at LEP2 [40,41]. The Tevatron reach depends very strongly on the final run II luminosity. Furthermore, the reach is very much affected by a suppression of the Higgs-boson production rate in the $H_i VV$ channel. Hence, it is unlikely that the Tevatron will be able to observe the lightest Higgs boson in the regions where the effective $H_1 VV$ coupling is suppressed. The search for the H_2 boson looks more promising. Indeed, for high luminosities available at a later stage of the collider, e.g. 30 fb^{-1} per experiment, the Tevatron-discovery reach of the Higgs-boson mass can be as high as 125 GeV for a SM production rate and 115 GeV if there is a 0.7 suppression factor.[†] From the results of Figs. 6–10, we can see that, as happens in the CP-conserving case [41], a high-luminosity Tevatron collider may be capable of covering most of the windows left open at LEP2.

In Fig. 15, we analyze the variation of the coupling of the charged Higgs bosons H^\pm to the lightest neutral Higgs boson H_1 and the W^\mp gauge bosons, for the same parameters as those considered in Fig. 6. The $H_1 H^+ W^-$ coupling may be defined from Eq. (5.2) without including the weak gauge-coupling factor $g_w/2$, i.e.

$$g_{H_1 H^+ W^-} = c_\beta O_{33} - s_\beta O_{23} + i O_{13}. \quad (5.12)$$

The $H_1 H^+ W^-$ coupling is relatively small when the coupling $H_1 Z Z$ is large, while it is enhanced when the coupling $H_1 Z Z$ is suppressed. On the other hand, a measure of CP violation in the $H_1 H^+ W^-$ vertex may be obtained by analyzing the CP-odd quantity $|\text{Im}(g_{H_1 H^+ W^-}^2)|/|g_{H_1 H^+ W^-}|^2$ (see also Fig. 15(b)). This CP-odd quantity shows a very interesting kinematic behaviour, as it can become of order 1 in large regions of the parameter space with $M_{H^\pm} \lesssim 300$ GeV. A consequence of large CP violation in the $H_1 H^+ W^-$ coupling is that the decay rates for $H^+ \rightarrow H_1 W^+$ and $H^- \rightarrow H_1 W^-$ may become very different [42].

In the following, we consider the interactions of the neutral Higgs fields with the fermions. These interactions may be obtained by the Lagrangian

$$\begin{aligned} \mathcal{L}_{H\bar{f}f} = & - \sum_{i=1}^3 H_{(4-i)} \left[\frac{g_w m_d}{2M_W c_\beta} \bar{d} (O_{2i} - i s_\beta O_{1i} \gamma_5) d \right. \\ & \left. + \frac{g_w m_u}{2M_W s_\beta} \bar{u} (O_{3i} - i c_\beta O_{1i} \gamma_5) u \right]. \end{aligned} \quad (5.13)$$

Obviously, the Higgs–fermion–fermion couplings are significant for the third-generation quarks, t and b . From Eq. (5.13), we readily see that the effect of CP-violating Higgs mixing is to induce a simultaneous coupling of H_i , with $i = 1, 2, 3$, to CP-even and CP-odd fermionic bilinears [43], e.g. to $\bar{u}u$ and $\bar{u}i\gamma_5 u$. This can lead to sizeable phenomena of CP

[†]These values rely on a combination of the $H_1 WW$ and $H_1 ZZ$ channel for both experiments [38], assuming that the total branching ratio into b quarks remains almost unchanged with respect to the SM value.

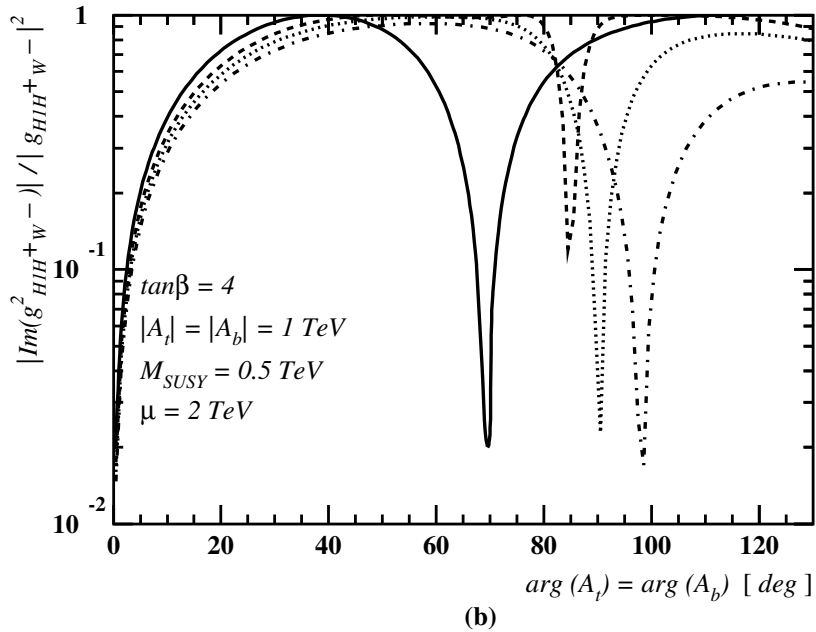
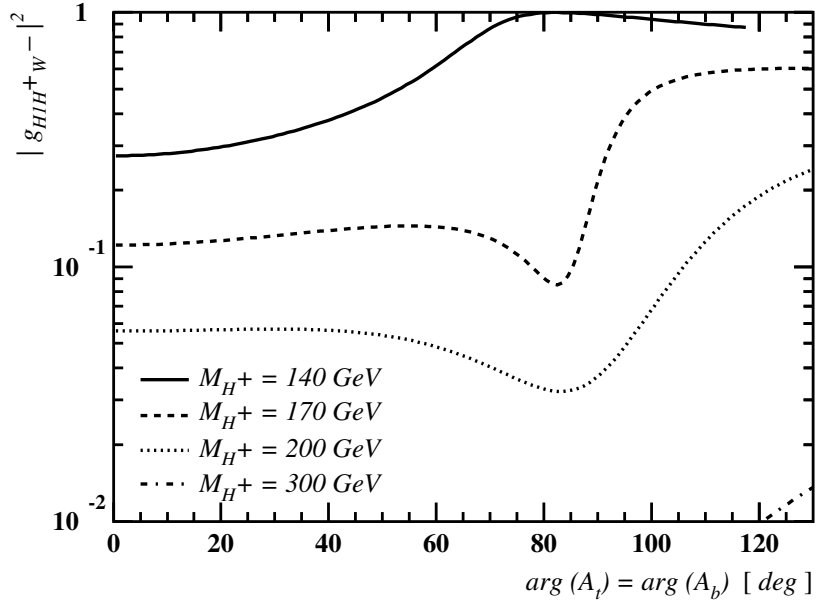


Figure 15: Numerical estimates of (a) $|g_{H_1 H^+ W^-}|^2$ and (b) $|\text{Im}(g_{H_1 H^+ W^-}^2)|/|g_{H_1 H^+ W^-}|^2$ as a function of $\arg(A_t)$. The definition of $g_{H_1 H^+ W^-}$ is given in Eq. (5.12).

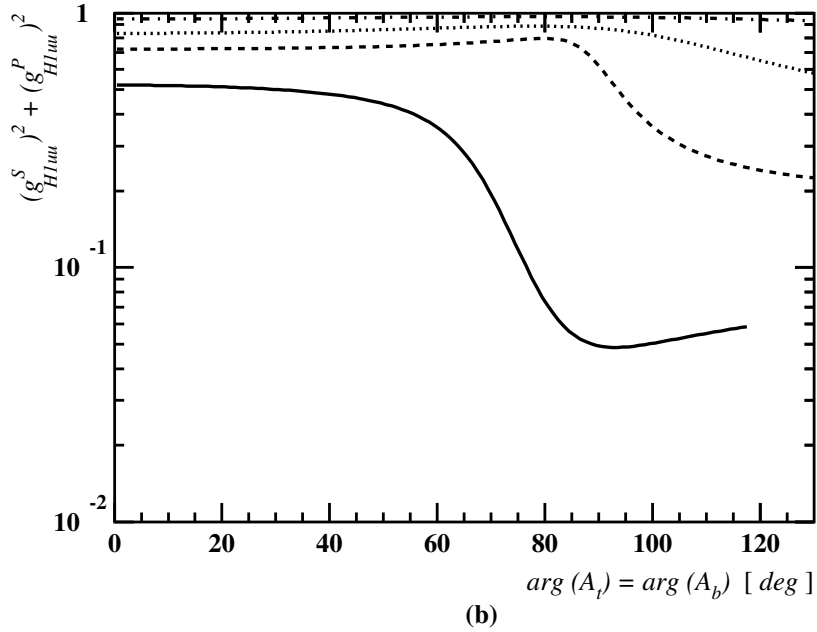
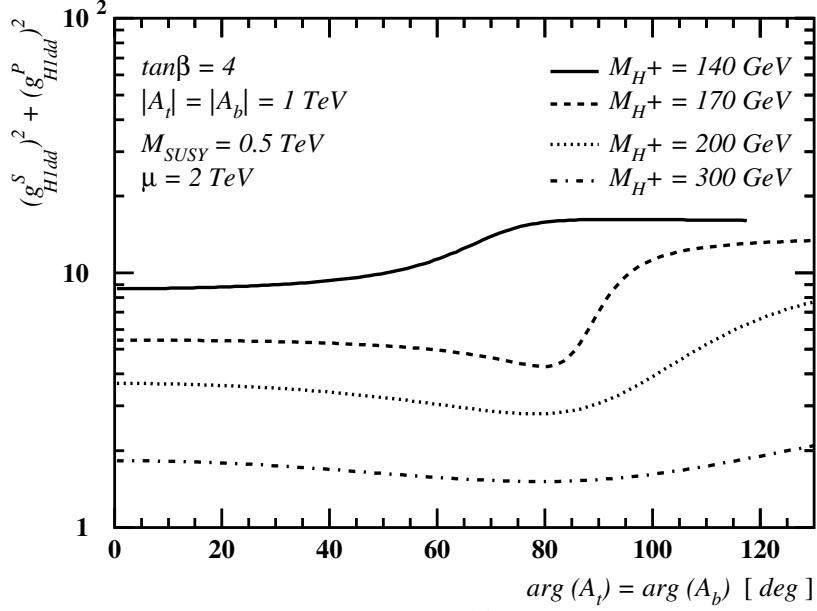


Figure 16: Numerical estimates of (a) $(g_{H_1 dd}^S)^2 + (g_{H_1 dd}^P)^2$ and (b) $(g_{H_1 uu}^S)^2 + (g_{H_1 uu}^P)^2$ versus $\arg(A_t)$. The definition of the couplings $g_{H_i dd}^{S,P}$ and $g_{H_i uu}^{S,P}$, with $i = 1, 2$, is given in Eq. (5.14).

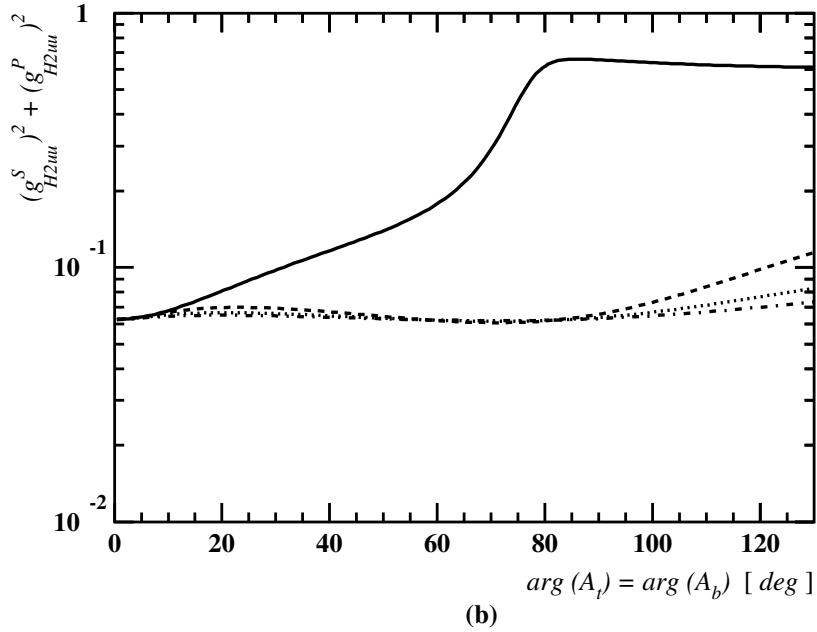
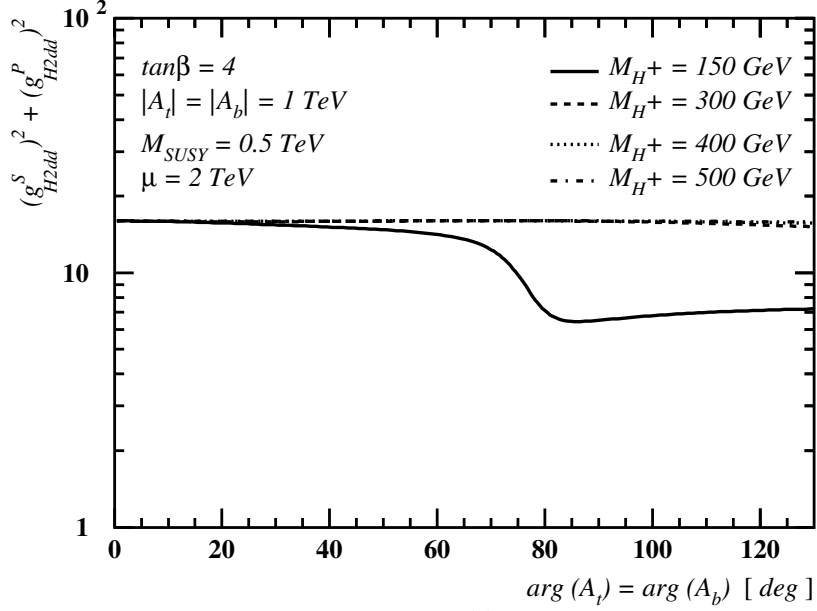


Figure 17: Numerical estimates of (a) $(g_{H2dd}^S)^2 + (g_{H2dd}^P)^2$ and (b) $(g_{H2uu}^S)^2 + (g_{H2uu}^P)^2$ as a function of $arg(A_t)$. The definition of the couplings $g_{H_i dd}^{S,P}$ and $g_{H_i uu}^{S,P}$, with $i = 1, 2$, is given in Eq. (5.14).

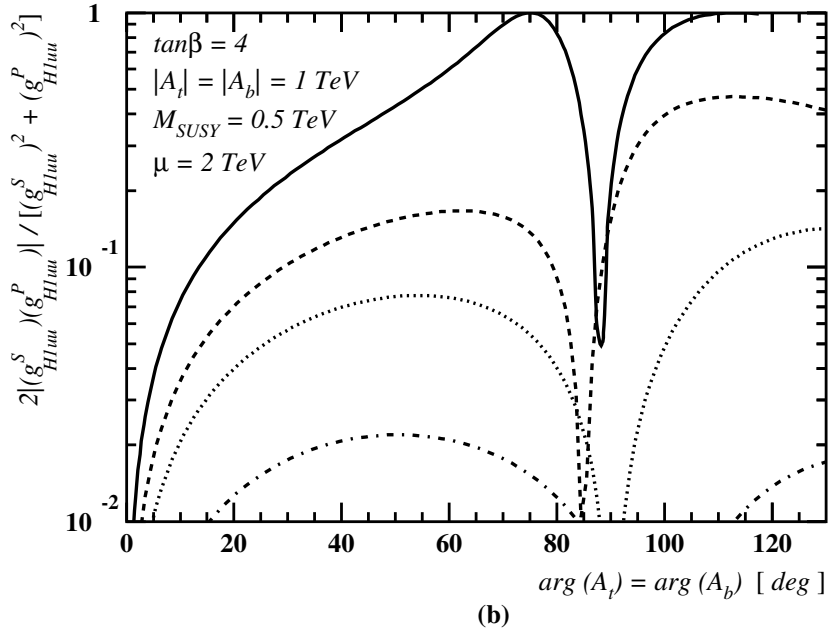
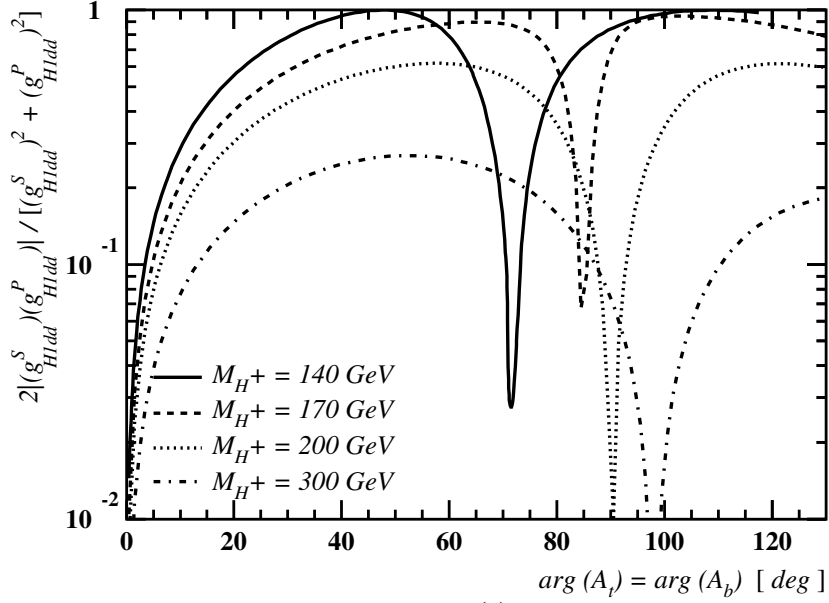


Figure 18: Numerical estimates of (a) $2|(g_{H_1 dd}^S)(g_{H_1 dd}^P)|/[(g_{H_1 dd}^S)^2 + (g_{H_1 dd}^P)^2]$ and (b) $2|(g_{H_1 uu}^S)(g_{H_1 uu}^P)|/[(g_{H_1 uu}^S)^2 + (g_{H_1 uu}^P)^2]$ as a function of $\arg(A_t)$. The definition of the couplings $g_{H_i dd}^{S,P}$ and $g_{H_i uu}^{S,P}$, with $i = 1, 2$, is given in Eq. (5.14)

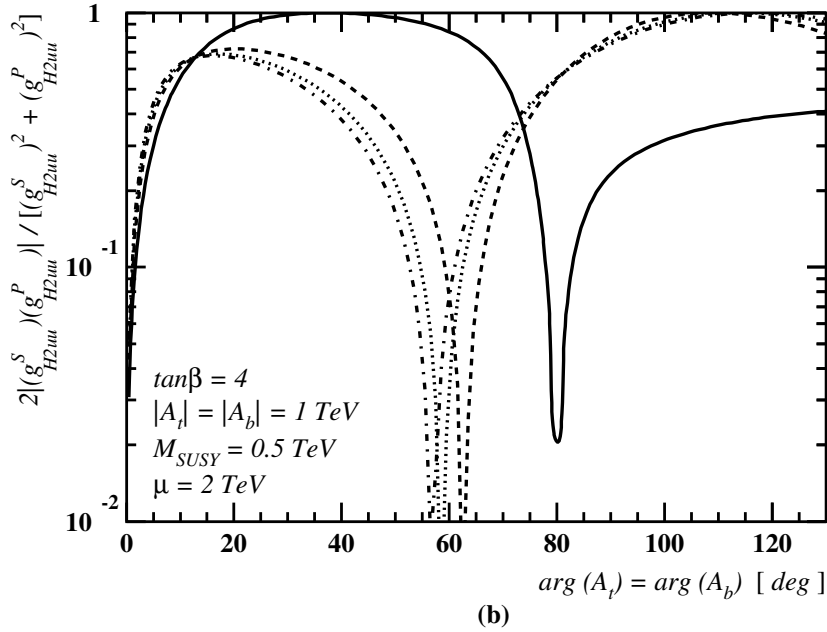
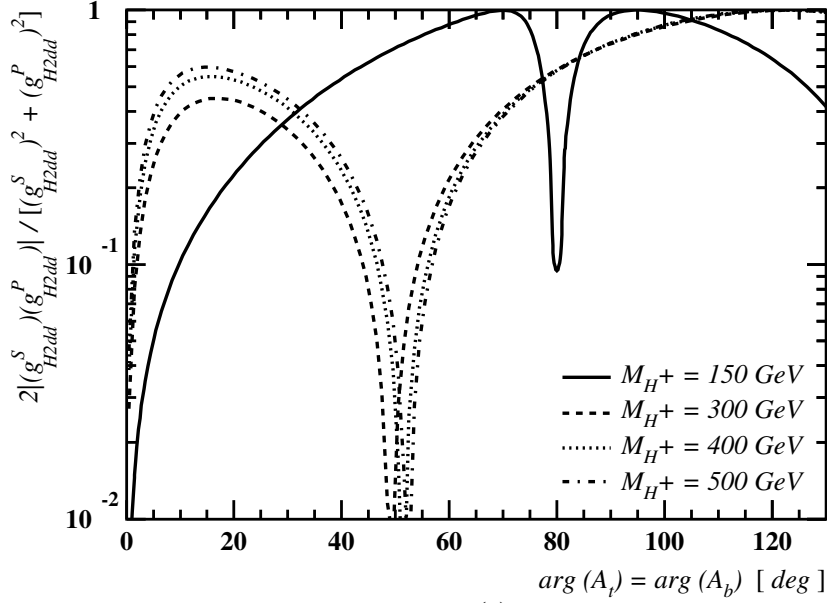


Figure 19: Numerical estimates of (a) $2|(g_{H_2dd}^S)(g_{H_2dd}^P)|/[(g_{H_2dd}^S)^2 + (g_{H_2dd}^P)^2]$ and (b) $2|(g_{H_2uu}^S)(g_{H_2uu}^P)|/[(g_{H_2uu}^S)^2 + (g_{H_2uu}^P)^2]$ as a function of $\arg(A_t)$. The definition of the couplings $g_{H_i dd}^{S,P}$ and $g_{H_i uu}^{S,P}$, with $i = 1, 2$, is given in Eq. (5.14).

violation in high-energy processes that involve decays of Higgs bosons into longitudinally polarized top-quark pairs [44].

For the discussion that follows, it proves convenient to define the following parameters:

$$\begin{aligned} g_{H_1uu}^S &= O_{33}/s_\beta, & g_{H_1uu}^P &= O_{13} \cot \beta, & g_{H_2uu}^S &= O_{32}/s_\beta, & g_{H_2uu}^P &= O_{12} \cot \beta, \\ g_{H_1dd}^S &= O_{23}/c_\beta, & g_{H_1dd}^P &= O_{13} \tan \beta, & g_{H_2dd}^S &= O_{22}/c_\beta, & g_{H_2dd}^P &= O_{12} \tan \beta. \end{aligned} \quad (5.14)$$

These parameters represent the scalar and pseudoscalar couplings of the Higgs bosons H_1 and H_2 to the up- and down-type fermions, normalized to the SM values. Then, the partial decay widths of H_1 and H_2 in the MSSM may be obtained by the SM ones, after multiplying the latter by the effective coupling factors $[(g_{H_1ff}^S)^2 + (g_{H_1ff}^P)^2]$ and $[(g_{H_2ff}^S)^2 + (g_{H_2ff}^P)^2]$ (with $f = u, d$), respectively. In Figs. 16 and 17, we plot the effective coupling factors as a function of $\arg(A_t)$. The behaviour observed is similar to the CP-conserving case. To be specific, the effective coupling factor related to the $H_i \bar{f} f$ coupling (with $i = 1, 2$) is close to the SM value, whenever the respective $H_i VV$ coupling approaches 1, while in the regions where the $H_i VV$ coupling is suppressed, the H_i coupling to down (up) fermions is enhanced (suppressed) by a factor $\tan \beta$ ($1/\tan \beta$).

One may now construct quantities that can provide a realistic measure of CP violation in the $H_1 \bar{f} f$ and $H_2 \bar{f} f$ couplings, i.e. $2|(g_{H_1ff}^S)(g_{H_1ff}^P)|/[(g_{H_1ff}^S)^2 + (g_{H_1ff}^P)^2]$. Figures 18 and 19 exhibit the dependence of these CP-violating quantities related to the H_1 and H_2 bosons, respectively, as a function of $\arg(A_t)$. Figure 18 reveals that the CP-violating component of the $H_1 \bar{f} f$ coupling is large only for relatively light charged Higgs-boson masses, $M_{H^+} \lesssim 180$ GeV. On the other hand, as can be seen from Fig. 19, the CP-violating component of the $H_2 \bar{f} f$ coupling may become of order 1 for a wide range of the parameter space, even for heavier charged Higgs-boson masses, e.g. $M_{H^+} \approx 500$ GeV.

Apart from the CP-violating effects generated by the radiative mixing of the Higgs fields which we consider here in detail, there may be important CP-violating effects induced by one-loop vertex corrections. In the leptonic sector, these corrections are generally small [45]. Because of the large Yukawa and colour-enhanced QCD interactions, however, the radiative corrections to the tree-level b -quark couplings to the Higgs bosons [46] may be important when the relevant Higgs-mass eigenstate has dominant components in the Higgs doublet Φ_2 [47,48] or, equivalently, when the matrix elements O_{2i} and $s_\beta O_{1i}$ related to the Higgs fields $H_{(4-i)}$ are small. In the CP-conserving case, the Higgs boson that couples predominantly to the gauge bosons always fulfils these properties [41], i.e. O_{12} and O_{13} are zero for the CP-even Higgs states in this case.

The general analytic expression for the effective Higgs-boson-bottom-quark coupling [41] may be obtained by considering the vertex graphs shown in Fig. 20. However, the mag-

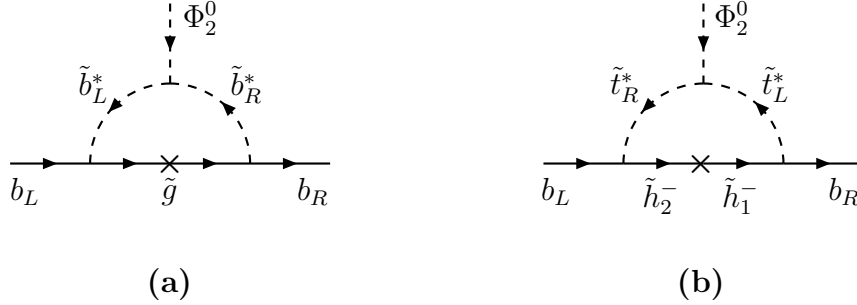


Figure 20: Feynman graphs mediated by the exchange of (a) gluinos \tilde{g} and (b) Higgsinos $\tilde{h}_{1,2}^-$ that give rise to an effective one-loop $\Phi_2^0 \bar{b} b$ coupling.

nitude of these corrections and the phases involved in these are strongly model-dependent. Furthermore, the gluino-exchange diagram in Fig. 20(a) usually represents the dominant contribution, which has a counterpart in the effective Higgs potential only at the two-loop level. To be precise, the effective one-loop Yukawa coupling of the b quark to the neutral field component of the Φ_2 doublet, $\Phi_2^0 = \phi_2 + ia_2$, is given by

$$\mathcal{L}_{\Phi_2^0 \bar{b} b} = \Delta h_b \Phi_2^0 \bar{b}_L b_R + \text{H.c.}, \quad (5.15)$$

with

$$\frac{\Delta h_b}{h_b} = \frac{2\alpha_s}{3\pi} m_{\tilde{g}} \mu I(m_{\tilde{b}_1}^2, m_{\tilde{b}_2}^2, |m_{\tilde{g}}|^2) + \frac{h_t^2}{16\pi^2} A_t \mu I(m_{\tilde{t}_1}^2, m_{\tilde{t}_2}^2, |\mu|^2), \quad (5.16)$$

where $\alpha_s = g_s^2/(4\pi)$ is the $SU(3)_c$ fine structure constant, h_t is the top Yukawa coupling, $m_{\tilde{b}_1}$ ($m_{\tilde{t}_1}$) and $m_{\tilde{b}_2}$ ($m_{\tilde{t}_2}$) are the mass eigenvalues of the scalar-bottom (top) quarks, and $I(a, b, c)$ is the one-loop function

$$I(a, b, c) = \frac{ab \ln(a/b) + bc \ln(b/c) + ac \ln(c/a)}{(a-b)(b-c)(a-c)}. \quad (5.17)$$

Note that the total bottom-mass corrections depend on the relative size of the gluino-mediated graphs to the Higgsino-mediated ones, shown in Figs. 20(a) and 20(b), respectively. Therefore, as was mentioned above, the two different quantum corrections strongly depend on the model under study. In fact, it is straightforward to introduce these quantum effects in the analysis of the Higgs couplings. Taking both CP-violating vertex and Higgs-mixing effects into consideration, the effective Lagrangian for the $H_i \bar{b} b$ couplings reads

$$\begin{aligned} \mathcal{L}_{H\bar{b}b}^{\text{eff}} = & - \sum_{i=1}^3 H_{(4-i)} \bar{b} \left\{ \left[h_b O_{2i} + \text{Re}(\Delta h_b) O_{3i} - \text{Im}(\Delta h_b) c_\beta O_{1i} \right] \right. \\ & \left. - i \left[h_b s_\beta O_{1i} - \text{Re}(\Delta h_b) c_\beta O_{1i} - \text{Im}(\Delta h_b) O_{3i} \right] \gamma_5 \right\} b, \end{aligned} \quad (5.18)$$

where

$$h_b = \frac{g_w m_b}{2M_W c_\beta |1 + (\Delta h_b/h_b) \tan \beta e^{i\xi}|} \quad (5.19)$$

and $\Delta h_b/h_b$ is given in Eq. (5.16).

As we have detailed above, the actual size of the CP-violating vertex effects depends both on ϕ_{CP} and $\arg(m_{\tilde{g}}\mu)$. The latter phase does not directly enter the calculation of the one-loop effective Higgs potential. To avoid excessive complication in the analysis, we have decided to present the results assuming that the vertex effects are very small, which is typically true for values of $\tan \beta \lesssim 4$, like the ones considered here. For larger values of $\tan \beta$, instead, these effects can no longer be ignored. However, a specific model is then needed in order to be able to determine their significance. For example, for an appropriate choice of SUSY-mass parameters and phases, the vertex effects can even be tuned to zero independently of the CP-violating Higgs-mixing effects.

6 Conclusions

We have performed a systematic study of the Higgs sector of the MSSM with explicit CP violation, and analyzed the main phenomenological implications of such a theory for direct searches of Higgs bosons at LEP2 and the upgraded Tevatron collider. In this general theoretical framework, the tree-level CP invariance of the MSSM Higgs potential is considered to be sizeably broken by loop graphs involving trilinear CP-violating couplings of the scalar top and bottom quarks to Higgs bosons [9]. These loop effects are taken into account by calculating the CP-violating RG-improved effective potential up to the next-to-leading order, in which two-loop leading logarithms of t -, b -Yukawa and QCD corrections have been included [6].

The analysis shows that the upper bound on the lightest Higgs-boson mass M_{H_1} obtained in the CP-violating MSSM is almost identical to that already derived in the CP-invariant theory, for both low and high $\tan \beta$ values. Nevertheless, the Higgs-sector CP non-conservation may drastically modify the couplings of the H_1 scalar to the Z and W bosons. In fact, the production rate of the H_1 boson is considerably affected at LEP2, for relatively light charged Higgs-boson masses, i.e. for $120 < M_{H^\pm} < 200$ GeV, and for small and intermediate values of $\tan \beta$, i.e. $2 \lesssim \tan \beta \lesssim 5$. For larger values of $\tan \beta$, the soft-CP-violating couplings of the third generation are severely constrained by the two-loop SUSY Barr-Zee-type contribution to the electron EDM [25], leading to much weaker CP-odd effects. Because of the drastic modification of the $H_1 ZZ$ and $H_1 H_2 Z$ couplings for low- and intermediate- $\tan \beta$ scenarios, we find that the current experimental lower bound

on the mass of the H_1 particle may be dramatically relaxed up to the 60-GeV level in the presence of large CP violation in the Higgs sector of the MSSM (see Fig. 8(b)). Therefore, a combined experimental analysis is required by considering all possible reactions that contain the two lightest neutral Higgs bosons, H_1 and H_2 , and the charged Higgs bosons H^\pm in the final state, which are produced either singly or in pairs. In this respect, the upgraded Tevatron collider and, to a greater extent, the LHC are the almost ideal places to explore more efficiently the parameter space of the CP-violating MSSM.

Another consequence of such a minimal SUSY scenario of explicit CP violation is that the mass splitting between the two heaviest Higgs bosons H_2 and H_3 may be of order 20% for heavy charged Higgs-boson masses, $M_{H^\pm} \approx 300$ GeV (see also Fig. 2(b)). This is in agreement with earlier results reported in [9]. Furthermore, we find that the strong mixing of the Higgs bosons may induce large CP violation in the vertices $H_1 H^\pm W^\mp$, $H_1 \bar{d}d$, $H_2 \bar{d}d$, etc., that could even be of order unity. Most interestingly, CP violation can be resonantly enhanced in high-energy reactions mediated by scalar–pseudoscalar transitions that involve the nearly degenerate H_2 and H_3 states, especially when the mass difference $M_{H_2} - M_{H_3}$ is comparable to the decay widths Γ_{H_2} and Γ_{H_3} [10]. Such resonant effects of CP violation may be tested at future high-energy colliders such as the LHC, NLC and the FMC [10,11,12,13,14,15]. Finally, the analysis presented in this paper clearly demonstrates that the MSSM with explicit CP violation in the Higgs sector constitutes an interesting theoretical framework, which will have a significant impact on B -meson decays, dark-matter searches and electroweak baryogenesis.

Acknowledgements

We wish to thank Jisuke Kubo for useful discussions, and Patrick Janot for providing us with experimental plots concerning Table 2.

Note added

While finalizing our paper, we became aware of two very recent works [49,50] that treat some of the topics we have been studying here. In [49], the author mainly concentrated on the effect of CP-violating Higgs mixing on the Higgs–fermion–fermion coupling for relatively low values of μ , i.e. $\mu = 250$ GeV, and $M_a = 200$ GeV. In this regime, CP violation in the sector of the lightest Higgs boson H_1 is small. Instead, we effectively consider smaller values of M_a , i.e. $120 \lesssim M_{H^+} \lesssim 180$ GeV, and higher values of μ , which can lead to significantly larger CP-violating effects in the H_1 sector. In this respect, our conclusions

differ from those presented in [49]; otherwise, we find agreement with the results regarding the $H_2\bar{f}f$ coupling. The authors of Ref. [50] discuss Higgs-boson production cross sections for a future e^+e^- NLC in a general CP-violating two-Higgs-doublet model. Here, instead, we are mainly interested in possible effects at LEP2 and the upgraded Tevatron collider, within the MSSM with radiatively induced CP violation in the Higgs sector. In addition to [49,50], we present analytic expressions for the Higgs-boson masses and mixing angles, and pay particular attention to the EDM constraints.

A Analytic expressions of quartic couplings

The dominant contribution of radiative interactions to quartic couplings comes from enhanced Yukawa couplings of the third generation. The relevant Lagrangians [51], including CP-violating sources, are given by

$$\begin{aligned}
-\mathcal{L}_{\text{soft}} &= \widetilde{M}_Q^2 \widetilde{Q}^\dagger \widetilde{Q} + \widetilde{M}_U^2 \widetilde{U}^* \widetilde{U} + \widetilde{M}_D^2 \widetilde{D}^* \widetilde{D} \\
&\quad + \left(h_b A_b \Phi_1^\dagger \widetilde{Q} \widetilde{D} - h_t A_t \Phi_2^T i\tau_2 \widetilde{Q} \widetilde{U} + \text{H.c.} \right), \tag{A.1}
\end{aligned}$$

$$\begin{aligned}
-\mathcal{L}_F &= h_b^2 |\Phi_1^\dagger \widetilde{Q}|^2 + h_t^2 |\Phi_2^T i\tau_2 \widetilde{Q}|^2 \\
&\quad - \left(\mu h_b \widetilde{Q}^\dagger \Phi_2 \widetilde{D}^* + \mu h_t \widetilde{Q}^\dagger i\tau_2 \Phi_1^* \widetilde{U}^* + \text{H.c.} \right) \\
&\quad - \left(h_b \widetilde{D}^* \Phi_1^T i\tau_2 + h_t \widetilde{U}^* \Phi_2^\dagger \right) \left(h_b i\tau_2 \Phi_1^* \widetilde{D} - h_t \Phi_2 \widetilde{U} \right), \tag{A.2}
\end{aligned}$$

$$\begin{aligned}
-\mathcal{L}_D &= \frac{g_w^2}{4} \left[2|\Phi_1^T i\tau_2 \widetilde{Q}|^2 + 2|\Phi_2^\dagger \widetilde{Q}|^2 - \widetilde{Q}^\dagger \widetilde{Q} (\Phi_1^\dagger \Phi_1 + \Phi_2^\dagger \Phi_2) \right] \\
&\quad + \frac{g'^2}{4} (\Phi_2^\dagger \Phi_2 - \Phi_1^\dagger \Phi_1) \left[\frac{1}{3} (\widetilde{Q}^\dagger \widetilde{Q}) - \frac{4}{3} (\widetilde{U}^* \widetilde{U}) + \frac{2}{3} (\widetilde{D}^* \widetilde{D}) \right], \tag{A.3}
\end{aligned}$$

$$-\mathcal{L}_{\text{fermions}} = h_b \left[\bar{b}_R(t_L, b_L) \Phi_1^* + \text{H.c.} \right] + h_t \left[\bar{t}_R(t_L, b_L) i\tau_2 \Phi_2 + \text{H.c.} \right], \tag{A.4}$$

with $\widetilde{Q}^T = (\tilde{t}_L, \tilde{b}_L)$, $\widetilde{U}^* = \tilde{t}_R$, $\widetilde{D}^* = \tilde{b}_R$. In addition, we also consider next-to-leading order QCD quantum corrections. These corrections have been computed in full detail in [17,18], and may easily be implemented in the analysis, as they form a CP-invariant subset of graphs by themselves.

Employing the interaction Lagrangians (A.1)–(A.4), it is straightforward to extend the two-loop analytic results in [6] to the case of CP violation. In this way, we find

$$\begin{aligned}
\lambda_1 &= -\frac{g_w^2 + g'^2}{8} \left(1 - \frac{3}{8\pi^2} h_b^2 t \right) \\
&\quad - \frac{3}{16\pi^2} h_b^4 \left[t + \frac{1}{2} X_b + \frac{1}{16\pi^2} \left(\frac{3}{2} h_b^2 + \frac{1}{2} h_t^2 - 8g_s^2 \right) (X_b t + t^2) \right] \\
&\quad + \frac{3}{192\pi^2} h_t^4 \frac{|\mu|^4}{M_{\text{SUSY}}^4} \left[1 + \frac{1}{16\pi^2} (9h_t^2 - 5h_b^2 - 16g_s^2) t \right], \tag{A.5}
\end{aligned}$$

$$\begin{aligned}
\lambda_2 &= -\frac{g_w^2 + g'^2}{8} \left(1 - \frac{3}{8\pi^2} h_t^2 t \right) \\
&\quad - \frac{3}{16\pi^2} h_t^4 \left[t + \frac{1}{2} X_t + \frac{1}{16\pi^2} \left(\frac{3}{2} h_t^2 + \frac{1}{2} h_b^2 - 8g_s^2 \right) (X_t t + t^2) \right] \\
&\quad + \frac{3}{192\pi^2} h_b^4 \frac{|\mu|^4}{M_{\text{SUSY}}^4} \left[1 + \frac{1}{16\pi^2} (9h_b^2 - 5h_t^2 - 16g_s^2) t \right], \tag{A.6}
\end{aligned}$$

$$\begin{aligned}
\lambda_3 &= -\frac{g_w^2 - g'^2}{4} \left[1 - \frac{3}{16\pi^2} (h_t^2 + h_b^2) t \right] \\
&\quad - \frac{3}{8\pi^2} h_t^2 h_b^2 \left[t + \frac{1}{2} X_{tb} + \frac{1}{16\pi^2} (h_t^2 + h_b^2 - 8g_s^2) (X_{tb} t + t^2) \right]
\end{aligned}$$

$$\begin{aligned}
& -\frac{3}{96\pi^2} h_t^4 \left(\frac{3|\mu|^2}{M_{\text{SUSY}}^2} - \frac{|\mu|^2 |A_t|^2}{M_{\text{SUSY}}^4} \right) \left[1 + \frac{1}{16\pi^2} (6h_t^2 - 2h_b^2 - 16g_s^2)t \right] \\
& -\frac{3}{96\pi^2} h_b^4 \left(\frac{3|\mu|^2}{M_{\text{SUSY}}^2} - \frac{|\mu|^2 |A_b|^2}{M_{\text{SUSY}}^4} \right) \left[1 + \frac{1}{16\pi^2} (6h_b^2 - 2h_t^2 - 16g_s^2)t \right], \tag{A.7}
\end{aligned}$$

$$\begin{aligned}
\lambda_4 = & \frac{g_w^2}{2} \left[1 - \frac{3}{16\pi^2} (h_t^2 + h_b^2)t \right] \\
& + \frac{3}{8\pi^2} h_t^2 h_b^2 \left[t + \frac{1}{2} X_{tb} + \frac{1}{16\pi^2} (h_t^2 + h_b^2 - 8g_s^2) (X_{tb}t + t^2) \right] \\
& -\frac{3}{96\pi^2} h_t^4 \left(\frac{3|\mu|^2}{M_{\text{SUSY}}^2} - \frac{|\mu|^2 |A_t|^2}{M_{\text{SUSY}}^4} \right) \left[1 + \frac{1}{16\pi^2} (6h_t^2 - 2h_b^2 - 16g_s^2)t \right] \\
& -\frac{3}{96\pi^2} h_b^4 \left(\frac{3|\mu|^2}{M_{\text{SUSY}}^2} - \frac{|\mu|^2 |A_b|^2}{M_{\text{SUSY}}^4} \right) \left[1 + \frac{1}{16\pi^2} (6h_b^2 - 2h_t^2 - 16g_s^2)t \right], \tag{A.8}
\end{aligned}$$

$$\begin{aligned}
\lambda_5 = & \frac{3}{192\pi^2} h_t^4 \frac{\mu^2 A_t^2}{M_{\text{SUSY}}^4} \left[1 - \frac{1}{16\pi^2} (2h_b^2 - 6h_t^2 + 16g_s^2)t \right] \\
& + \frac{3}{192\pi^2} h_b^4 \frac{\mu^2 A_b^2}{M_{\text{SUSY}}^4} \left[1 - \frac{1}{16\pi^2} (2h_t^2 - 6h_b^2 + 16g_s^2)t \right], \tag{A.9}
\end{aligned}$$

$$\begin{aligned}
\lambda_6 = & -\frac{3}{96\pi^2} h_t^4 \frac{|\mu|^2 \mu A_t}{M_{\text{SUSY}}^4} \left[1 - \frac{1}{16\pi^2} \left(\frac{7}{2} h_b^2 - \frac{15}{2} h_t^2 + 16g_s^2 \right) t \right] \\
& + \frac{3}{96\pi^2} h_b^4 \frac{\mu}{M_{\text{SUSY}}} \left(\frac{6A_b}{M_{\text{SUSY}}} - \frac{|A_b|^2 A_b}{M_{\text{SUSY}}^3} \right) \left[1 - \frac{1}{16\pi^2} \left(\frac{1}{2} h_t^2 - \frac{9}{2} h_b^2 + 16g_s^2 \right) t \right], \tag{A.10}
\end{aligned}$$

$$\begin{aligned}
\lambda_7 = & -\frac{3}{96\pi^2} h_b^4 \frac{|\mu|^2 \mu A_b}{M_{\text{SUSY}}^4} \left[1 - \frac{1}{16\pi^2} \left(\frac{7}{2} h_t^2 - \frac{15}{2} h_b^2 + 16g_s^2 \right) t \right] \\
& + \frac{3}{96\pi^2} h_t^4 \frac{\mu}{M_{\text{SUSY}}} \left(\frac{6A_t}{M_{\text{SUSY}}} - \frac{|A_t|^2 A_t}{M_{\text{SUSY}}^3} \right) \left[1 - \frac{1}{16\pi^2} \left(\frac{1}{2} h_b^2 - \frac{9}{2} h_t^2 + 16g_s^2 \right) t \right], \tag{A.11}
\end{aligned}$$

where $t = \ln(M_{\text{SUSY}}^2/\bar{m}_t^2)$ and

$$h_t = \frac{\sqrt{2} m_t(\bar{m}_t)}{v \sin \beta}, \quad h_b = \frac{\sqrt{2} m_b(\bar{m}_t)}{v \cos \beta}, \tag{A.12}$$

$$\begin{aligned}
X_t &= \frac{2|A_t|^2}{M_{\text{SUSY}}^2} \left(1 - \frac{|A_t|^2}{12M_{\text{SUSY}}^2} \right), \\
X_b &= \frac{2|A_b|^2}{M_{\text{SUSY}}^2} \left(1 - \frac{|A_b|^2}{12M_{\text{SUSY}}^2} \right), \\
X_{tb} &= \frac{|A_t|^2 + |A_b|^2 + 2\text{Re}(A_b^* A_t)}{2M_{\text{SUSY}}^2} - \frac{|\mu|^2}{M_{\text{SUSY}}^2} - \frac{||\mu|^2 - A_b^* A_t|^2}{6M_{\text{SUSY}}^4}. \tag{A.13}
\end{aligned}$$

In Eq. (A.12), \bar{m}_t is the top-quark pole mass, which is related to the on-shell running mass m_t through

$$m_t(\bar{m}_t) = \frac{\bar{m}_t}{1 + \frac{4}{3\pi} \alpha_s(\bar{m}_t)}. \tag{A.14}$$

It is important to remark that the above expressions are not equivalent to the ones that

would be obtained by taking the expressions given in Ref. [6], and considering all mixing parameters to be complex. If this were done, incorrect results would be obtained.

The RG analysis under consideration assumes a single step decoupling of the scalar-quark fields. This assumption is only valid if the mass splitting among the scalar-quark mass eigenstates is relatively small [6]. Specifically, the expansion becomes more trustworthy if

$$\frac{m_{\tilde{t}_1}^2 - m_{\tilde{t}_2}^2}{m_{\tilde{t}_1}^2 + m_{\tilde{t}_2}^2} \lesssim 0.5, \quad (\text{A.15})$$

where $m_{\tilde{t}_1}^2$ and $m_{\tilde{t}_2}^2$ are the squared mass eigenvalues of the scalar-top quarks. This last restriction also applies to other Higgs-mass analyses that have been performed at the next-to-leading order [4,5,6]. If one assumes that the approximate inequality (A.15) holds true, the scale M_{SUSY}^2 may then be safely defined as the arithmetic average of the scalar-top mass eigenvalues squared,

$$M_{\text{SUSY}}^2 = \frac{1}{2} (m_{\tilde{t}_1}^2 + m_{\tilde{t}_2}^2). \quad (\text{A.16})$$

One should bear in mind that our RG analysis also relies on an expansion of the effective Higgs potential up to operators of dimension 4. The contribution of higher-dimensional operators may only be neglected if $2|m_t A_t| \lesssim M_{\text{SUSY}}^2$ and $2|m_t \mu| \lesssim \tan \beta M_{\text{SUSY}}^2$. Moreover, in the high $\tan \beta$ regime, in which the bottom-Yukawa interactions become more relevant, we have assumed that the scalar-bottom masses are of the order of the scalar-top ones and that similar bounds on their respective mixing mass parameters are fulfilled. Observe that, in order to evaluate Higgs-boson pole masses, Higgs-vacuum-polarization contributions should be included in the calculation. In general, for our choice of the renormalization scale, the vacuum-polarization contributions are small. These contributions would only be necessary in a calculation of Higgs-boson masses that goes beyond the approximation presented here. Therefore, the present approach is very analogous to that studied in Ref. [52] in the MSSM framework with CP-invariant Higgs potential.

The computation of the Higgs-boson mass-matrix elements considered here and in [6] is still affected by theoretical uncertainties, most noticeably, those associated with two-loop, finite threshold corrections to the effective quartic couplings of the Higgs potential. Recently, a partial, diagrammatic, two-loop calculation of the mass of the lightest CP-even Higgs boson has been carried out [53]. In the limit of large M_{H^+} , the additional two-loop threshold corrections lead to a slight modification of the dependence of the lightest CP-even Higgs-boson mass on the scalar-top mixing parameters. For instance, although the upper bound on the lightest CP-even Higgs-boson mass for TeV scalar-quark masses is approximately equal to that obtained through next-to-leading order, which is also the approach we followed in the present work, the upper bound on the Higgs-boson mass is

reached for slightly different values of $|\tilde{A}_t|$, i.e. $|\tilde{A}_t| \simeq 2M_{\text{SUSY}}$ instead of $|\tilde{A}_t| = \sqrt{6} M_{\text{SUSY}}$, with a weak dependence on the sign of \tilde{A}_t . Similar results were obtained by means of a two-loop calculation of the effective potential [54]. Nevertheless, a complete diagrammatic analysis of the two-loop corrections induced by the t -Yukawa coupling, which are included at the leading-logarithmic level in our computation, is still lacking.

References

- [1] LEP Committee, 12 November, 1998, CERN/LEPC 98-9. The experimental collaborations at CERN report the following lower mass bounds on the SM Higgs boson at 95% CL: 95.5 GeV (L3) [<http://hpl3sn02.cern.ch/analysis/latestresults.html>], 94 GeV (OPAL) [<http://www1.cern.ch/Opal/plots/plane/lepc98.html>], 94.1 GeV (DELPHI) [<http://delphiwww.cern.ch/delfigs/figures/figures.html>]; 90.4 GeV (ALEPH) [<http://alephwww.cern.ch/ALPUB/oldconf/oldconf99.html>].
- [2] For recent analyses, see for instance J. Erler and P. Langacker, to appear in Proceedings of the “5th International Wein Symposium: A Conference on Physics Beyond the Standard Model (WEIN 98),” Santa Fe, NM, 14–21 June 1998, hep-ph/9809352; G. Degrassi, P. Gambino, M. Passera and A. Sirlin, Phys. Lett. **B418** (1998) 209; G. D’Agostini and G. Degrassi, hep-ph/9902226
- [3] For a review, see, J.F. Gunion, H.E. Haber, G. Kane and S. Dawson, “The Higgs Hunters Guide,” (Addison-Wesley, Reading, MA, 1990).
- [4] M.S. Berger, Phys. Rev. **D41** (1990) 225; Y. Okada, M. Yamaguchi and T. Yanagida, Prog. Theor. Phys. **85** (1991) 1; Phys. Lett. **B262** (1991) 54; H.E. Haber and R. Hempfling, Phys. Rev. Lett. **66** (1991) 1815; J. Ellis, G. Ridolfi and F. Zwirner, Phys. Lett. **B257** (1991) 83; R. Barbieri, M. Frigeni and F. Caravaglios, Phys. Lett. **B258** (1991) 167; P.H. Chankowski, Warsaw preprint 1991, IFT-7-91 (unpublished); J.R. Espinosa and M. Quirós, Phys. Lett. **B266** (1991) 389; J.L. Lopez and D.V. Nanopoulos, Phys. Lett. **B266** (1991) 397; M. Carena, K. Sasaki and C.E.M. Wagner, Nucl. Phys. **B381** (1992) 66; P.H. Chankowski, S. Pokorski and J. Rosiek, Phys. Lett. **B281** (1992) 100; Nucl. Phys. **B423** (1994) 437; D.M. Pierce, A. Papadopoulos and S.B. Johnson, Phys. Rev. Lett. **68** (1992) 3678; A. Brignole, Phys. Lett. **B281** (1992) 284; V. Barger, M.S. Berger and P. Ohmann, Phys. Rev. **D49** (1994) 4908; G.L. Kane, C. Kolda, L. Roszkowski and J.D. Wells, Phys. Rev. **D49** (1994) 6173; R. Hempfling and A.H. Hoang, Phys. Lett. **B331** (1994) 99; P. Langacker and N. Polonsky, Phys. Rev. **D50** (1994) 2199.
- [5] H.E. Haber and R. Hempfling, Phys. Rev. **D48** (1993) 4280.
- [6] M. Carena, J.R. Espinosa, M. Quirós and C.E.M. Wagner, Phys. Lett. **B355** (1995) 209.

- [7] J. Ellis, T. Falk, K. Olive and M. Schmitt, Phys. Lett. **B388** (1996) 97; Phys. Lett. **B413** (1997) 355; S.A. Abel and B.C. Allanach, Phys. Lett. **B431** (1998) 339; J.A. Casas, J.R. Espinosa and H.E. Haber, Nucl. Phys. **B526** (1998) 3.
- [8] M. Carena, P. Chankowski, S. Pokorski and C.E.M. Wagner, Phys. Lett. **B441** (1998) 205.
- [9] A. Pilaftsis, Phys. Lett. **B435** (1998) 88; Phys. Rev. **D58** (1998) 096010.
- [10] A. Pilaftsis, Nucl. Phys. **B504** (1997) 61.
- [11] A. Pilaftsis and M. Nowakowski, Int. J. Mod. Phys. **A9** (1994) 1097; G. Cvetič, Phys. Rev. **D48** (1993) 5280; B. Grzadkowski, Phys. Lett. **B338** (1994) 71.
- [12] C.A. Boe, O.M. Ogreid, P. Osland and J.-Z. Zhang, hep-ph/9811505; see also A. Skjold and P. Osland, Nucl. Phys. **B453** (1995) 3.
- [13] W. Bernreuther, A. Brandenburg and M. Flesch, Phys. Rev. **D56** (1997) 90; hep-ph/9812387.
- [14] A. Pilaftsis, Phys. Rev. Lett. **77** (1996) 4996.
- [15] S.-Y. Choi and M. Drees, Phys. Rev. Lett. **81** (1998) 5509.
- [16] M. Carena, M. Quirós and C.E.M. Wagner, Phys. Lett. **B380** (1996) 81; Nucl. Phys. **B524** (1998) 3; J.R. Espinosa, Nucl. Phys. **B475** (1996) 273; D. Delepine, J.M. Gerard, R. Gonzalez-Felipe and J. Weyers, Phys. Lett. **B386** (1996) 183; A. Riotto, Phys. Rev. **D53** (1996) 5834; J.R. Espinosa and B. De Carlos, Nucl. Phys. **B503** (1997) 24; D. Bödeker, P. John, M. Laine and M.G. Schmidt, Nucl. Phys. **B497** (1997) 387; M. Carena, M. Quiros, A. Riotto, I. Vilja and C.E.M. Wagner, Nucl. Phys. **B503** (1997) 387; J.M. Cline, M. Joyce and M. Kainulainen, Phys. Lett. **B417** (1998) 79; M. Laine and K. Rummukainen, Phys. Rev. Lett. **80** (1998) 5259; Nucl. Phys. **B535** (1998) 423; J.M. Cline and G.D. Moore, Phys. Rev. Lett. **81** (1998) 3317; M. Losada, Nucl. Phys. **B537** (1999) 3; K. Funakubo, hep-ph/9809517; J. Grant and M. Hindmarsh, hep-ph/9811289; M. Laine and K. Rummukainen, hep-ph/9811369; A.B. Lahanas, V.C. Spanos and V. Zarikas, hep-ph/9812535.
- [17] J. Kodaira, Y. Yasui and K. Sasaki, Phys. Rev. **D50** (1994) 7035.
- [18] J.A. Casas, J.R. Espinosa, M. Quirós and A. Riotto, Nucl. Phys. **B436** (1995) 3; (E) **B439** (1995) 466.

- [19] J. Ellis, S. Ferrara and D.V. Nanopoulos, Phys. Lett. **B114** (1982) 231; W. Buchmüller and D. Wyler, Phys. Lett. **B121** (1983) 321; J. Polchinski and M. Wise, Phys. Lett. **B125** (1983) 393; F. del Aguila, M. Gavela, J. Grifols and A. Mendez, Phys. Lett. **B126** (1983) 71; D.V. Nanopoulos and M. Srednicki, Phys. Lett. **B128** (1983) 61.
- [20] M. Dugan, B. Grinstein and L. Hall, Nucl. Phys. **B255** (1985) 413.
- [21] T. Falk, K.A. Olive and M. Srednicki, Phys. Lett. **B354** (1995) 99; T. Falk and K.A. Olive, hep-ph/9806236.
- [22] Y. Kizukuri and N. Oshimo, Phys. Rev. **D46** (1992) 3025.
- [23] T. Ibrahim and P. Nath, Phys. Lett. **B418** (1998) 98; M. Brhlik, G.J. Good and G.L. Kane, hep-ph/9810457.
- [24] See, for example, S.A. Abel and J.-M. Frère, Phys. Rev. **D55** (1997) 1623, and references therein.
- [25] D. Chang, W.Y. Keung and A. Pilaftsis, Phys. Rev. Lett. **82** (1999) 900.
- [26] G.C. Branco and M.N. Rebelo, Phys. Lett. **B160** (1985) 117; J. Liu and L. Wolfenstein, Nucl. Phys. **B289** (1987) 1.
- [27] N. Maekawa, Phys. Lett. **B282** (1992) 387.
- [28] A. Pomarol, Phys. Lett. **B287** (1992) 331; N. Haba, Phys. Lett. **B398** (1997) 305.
- [29] O.C.W. Kong and F.-L. Lin, Phys. Lett. **B419** (1998) 217.
- [30] S. Weinberg, Phys. Rev. Lett. **63** (1989) 2333; E. Braaten, C.S. Li and T.C. Yuan, Phys. Rev. Lett. **64** (1990) 1709.
- [31] S.M. Barr and A. Zee, Phys. Rev. Lett. **65** (1990) 21.
- [32] C. Caso et al. (Particle Data Group), Eur. Phys. J. **C3** (1998) 1.
- [33] K. Abdullah, C. Carlberg, E.D. Commins, H. Gould and S.B. Ross, Phys. Rev. Lett. **65** (1990) 2347.
- [34] E.D. Commins, S.B. Ross, D. DeMille and B.C. Regan, Phys. Rev. **A50** (1994) 2960.
- [35] I.S. Altarev et al., Phys. Atom. Nucl. **59** (1996) 1152.
- [36] W. Fischler, S. Paban and S. Thomas, Phys. Lett. **B289** (1992) 373, and references therein.

- [37] M. Carena, P. Zerwas, and convenors of the Higgs Physics Working Group, in Physics at LEP2, eds. G. Altarelli, T. Sjöstrand and F. Zwirner, (Report CERN 96-01, Geneva 1996), Vol. 1.
- [38] M. Carena and J. Lykken, “Report of the Physics at Run II Supersymmetry/Higgs Workshop,” Fermilab, 1999, eds., in preparation.
- [39] A. Méndez and A. Pomarol, Phys. Lett. **B272** (1991) 313; J.F. Gunion, B. Grzadkowski, H.E. Haber and J. Kalinowski, Phys. Rev. Lett. **79** (1997) 982.
- [40] H. Baer, B.W. Harris and X. Tata, Phys. Rev. **D59** (1999) 015003.
- [41] M. Carena, S. Mrenna and C.E.M. Wagner, hep-ph/9808312, to be published in Phys. Rev. D.
- [42] L. Lavoura, Phys. Rev. **D51** (1995) 5256.
- [43] N.G. Deshpande and E. Ma, Phys. Rev. **D16** (1977) 1583; Phys. Rev. **D18** (1978) 2574.
- [44] D. Chang and W.-Y. Keung, Phys. Lett. **B305** (1993) 261; D. Chang, W.-Y. Keung and I. Phillips, Phys. Rev. **D48** (1993) 3225.
- [45] K.S. Babu, C. Kolda, J. March-Russell and F. Wilczek, Phys. Rev. **D59** (1999) 016004.
- [46] E. Ma, Phys. Rev. **D39** (1989) 1922.
- [47] R. Hempfling, Phys. Rev. **D49** (1994) 6168; L. Hall, R. Rattazzi and U. Sarid, Phys. Rev. **D50** (1994) 7048; M. Carena, M. Olechowski, S. Pokorski and C.E.M. Wagner, Nucl. Phys. **B426** (1994) 269; D. Pierce, J. Bagger, K. Matchev and R. Zhang, Nucl. Phys. **B491** (1997) 3.
- [48] J.A. Coarasa, R.A. Jimenez and J. Sola, Phys. Lett. **B389** (1996) 312; R.A. Jimenez and J. Sola, Phys. Lett. **B389** (1996) 53; K.T. Matchev and D.M. Pierce, Phys. Lett. **B445** (1999) 331; P.H. Chankowski, J. Ellis, M. Olechowski and S. Pokorski, hep-ph/9808275; K.S. Babu and C. Kolda, hep-ph/9811308.
- [49] D.A. Demir, hep-ph/9901389.
- [50] B. Grzadkowski, J.F. Gunion and J. Kalinowski, hep-ph/9902308.
- [51] J.F. Gunion and H.E. Haber, Nucl. Phys. **B272** (1986) 1; (E) **B402** (1993) 567.

- [52] M. Carena, M. Quiros and C.E.M. Wagner, Nucl. Phys. **B461** (1996) 407; H.E. Haber, R. Hempfling and A.H. Hoang, Z. Phys. **C75** (1997) 539.
- [53] S. Heinemeyer, W. Hollik and G. Weiglein, Phys. Rev. **D58** (1998) 091701; Phys. Lett. **B440** (1998) 96.
- [54] R.-J. Zhang, Phys. Lett. **B447** (1999) 89.